SOUTHERN CALIFORNIA EDISON COMPANY

SAN ONOFRE NUCLEAR GENERATING STATION

PRIMARY REACTOR CONTAINMENT STRUCTURAL INTEGRITY TEST

SAN ONOFRE NUCLEAR GENERATING STATION

UNIT 2

CONTAINMENT STRUCTURAL INTEGRITY TEST

FINAL REPORT

PREPARED BY

BECHTEL POWER CORPORATION

FEBRUARY, 1981

TABLE OF CONTENTS

LIST OF FIGURES

LIST OF FIGURES (Cont'd)

FIGURE NO.

1. INTRODUCTION

The Unit 2 Containment Structural Integrity Test was conducted in conjunction with the Preoperational Integrated Leakage Rate Test during the time period November 29, 1980, through December 4, 1980. The primary purpose of the structural integrity test was to verify the design and the structural integrity of the containment structure by imposing an internal pressure of 115 percent of design pressure for a period of not less than two hours.

In order to accomplish the intended test purpose, specialized measuring devices were employed on and in the containment structure to provide the data needed to evaluate structural response during pressurization and depressurization. The test was conducted in accordance with written procedure 2PE-101-03 detailing test requirements and instructions for acquiring test data (Reference a). The test procedure incorporated the commitments contained in the Final Safety Analysis Report (Reference b) and generally conformed to the guidelines set forth in USNRC Regulatory Guide 1.18 (Reference c) and the NRC approved Bechtel Topical Report, BC-TOP-5 (Reference d).

2. SUMMARY AND CONCLUSIONS

The structural integrity test consisted of (1) proof of containment ability to contain 115 percent of design pressure and (2) measurement of structural response to changes in internal pressure. Test measurements include gross structural deformation, concrete strains/temperatures, and concrete crack growth. Measurement points were located along typical sections of the containment structure, at thickened sections and at discontinuities. Test measurements were recorded at specific stages during the pressurization cycle.

The containment structure withstood the test pressure of 69.4 psig with no indications of structural overloading. Measured values of deformation, strain and concrete crack growth were within design allowable values. Strains and deformations generally remained within the elastic range.

Deformation and strain generally varied linearly with pressure through 69.4 psig. Small residuals were measured at the completion of depressurization which reflected the delayed elastic response of the concrete under the sustained loading - about 90 hours from the start of the pressurization to start of final blowdown. The delayed response occurred slowly and was not noticeable during the hold periods associated with the integrated leakage rate test.

Deformation and strain at 69.4 psig were reasonably close to the values predicted for maximum test pressure. Radial movements of the containment shell showed considerable variation between the monitored azimuths at each elevation; however, the net diametral growth across the three instrumented diameters was consistent at all elevations and is both linear with pressure and reasonably close to expected values. The variations in radial displacement with azimuth are attributed to (1) slight lateral displacements of the interior structures used as frames of reference for radial measurements and/or (2) the normal tendency of the single curvature cylindrical surface of the shell to round up under internal pressure. Measured vertical growth of the wall was as predicted. Vertical movements of the dome showed the smooth trend expected for the doubly curved spherical surface. The measured values - referenced to the tops of the steam generator walls were between the values predicted for a rigid base mat and those predicted for a conservatively modelled, flexible mat. Radial movements near the equipment opening were consistent with values expected based on movements of the regular areas of the cylinder wall.

Measured strains were influenced by the variations in containment wall thermal gradient since the measuring devices respond to the combination of strains induced by both pressure and thermal stresses. Allowing for the magnitude of expected thermal gradients places most measured strains within a reasonable range of predicted values. Measured strains at the wall/base mat juncture departed from predicted values by amounts greater than those attributable to temperature gradient and measurement error. This was expected since measured strains in this zone of high strain gradient are very sensitive to both exact position and gage length of the measuring devices.

2. (Continued)

Surface cracks observed on the concrete within and adjacent to the seven surveillance areas increased in width by only minor amounts during containment pressurization. The largest recorded increases were well below the acceptance limit of 0.06 inches.

Overall, the results of the structural integrity test provide direct experimental evidence that the containment structure can contain the design internal pressure with a sufficient margin of safety and that the gross response to pressure is within allowable limits.

3. CONTAINMENT STRUCTURE AND PRESSURIZATION

The containment is a post-tensioned, reinforced concrete structure designed to contain any accidental release of radioactivity from the reactor coolant system as defined in the Final Safety Analysis Report (Reference b). The containment is designed for an internal accident pressure pressure of 60 psig.

The structure consists of a post-tensioned, reinforced concrete cylindrical wall and hemispherical dome connected to and supported by a massive reinforced concrete base slab as shown in Figure 3-1. The cylinder wall and dome thickness is increased at three equally spaced locations to form vertical buttresses for prestressing tendon end anchorage. Reinforced openings in the cylinder wall are provided for equipment and personnel access as well as for electrical and mechanical system penetration. The containment is posttensioned by two groups of stranded tendons. The circumferential group, which consists of overlapping tendons anchored at buttresses 240° apart, prestresses the wall and lower half of the dome in the hoop direction. The vertical group, which consists of inverted U tendons anchored in the tendon access gallery, prestresses the wall and dome in the vertical direction. The entire interior surface of the structure is lined with 1/4 inch thick welded steel plate which serves as a leak tight membrane.

Principal dimensions of the containment structure are:

Inside Diameter	150 ft.
Inside Height of Cylinder	97 ft.
Radius of Spherical Dome	75 ft.
Vertical Wall Thickness	4 ft., 4 in.
Dome Thickness	Tapering from 4 ft. 4 in. at Springline to 3 ft. 9 in. at Apex
Foundation Slab Thickness	9 ft.

The containment structure was pressurized pneumatically to verify the required structural integrity and to measure gross leakage. The pressure cycle is shown in Figure 3-2. The proof pressure of 69.4 psig, equal to 1.15 times design pressure (Reference b), plus a tolerance of 0.4 psig, was specified to assure that the containment structure has sufficient reserve strength. Proof pressure was held for a period of two hours to record structural response data. Additional plateaus were included in the cycle to permit constant presure data acquisition at various intermediate

3. (Continued)

pressure levels. Pressure was held constant for a minimum of one hour during these plateaus. The long plateaus at 46 and 57 psig were as required to complete the integrated leakage rate test.

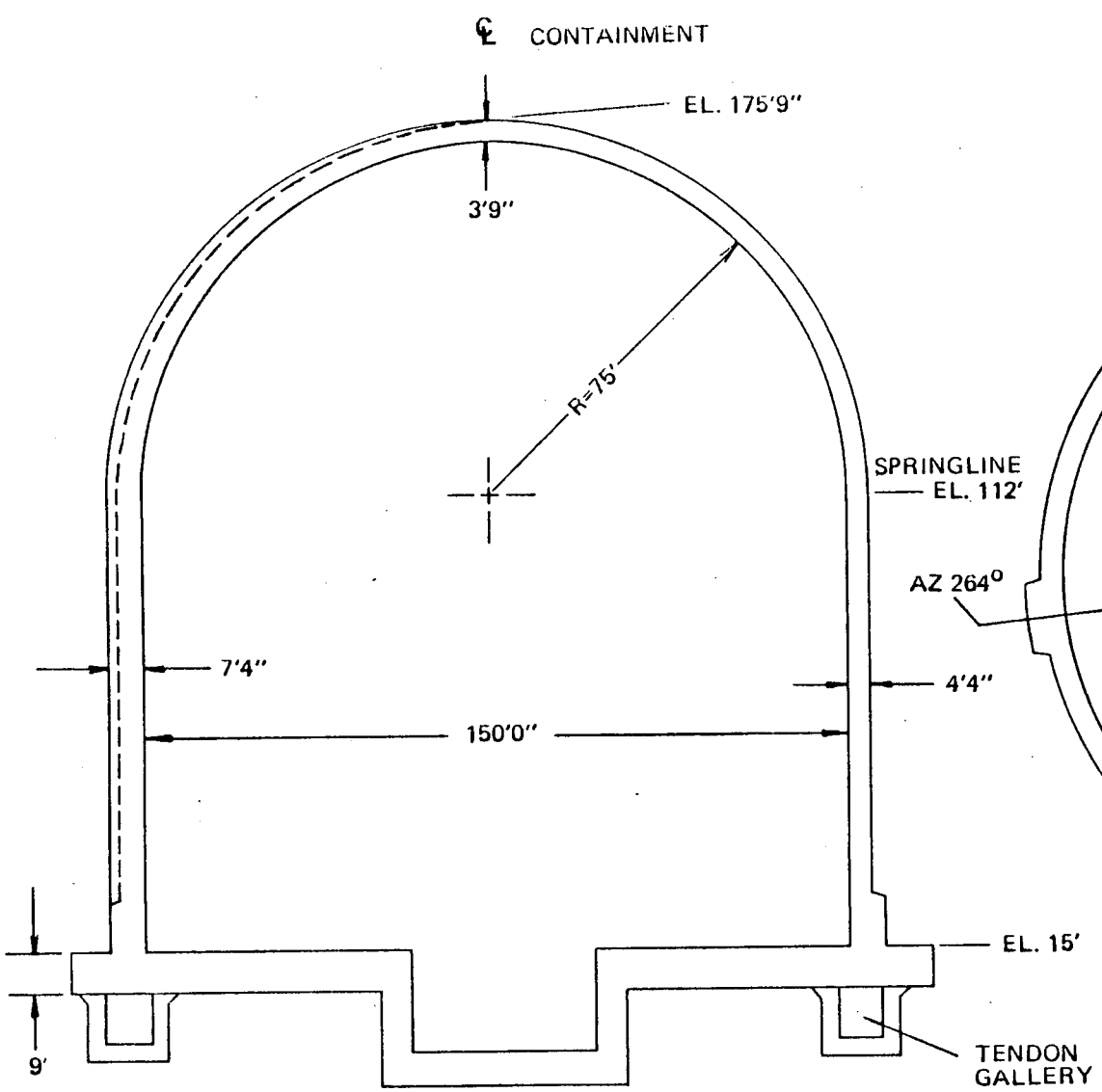

SECTION A-A

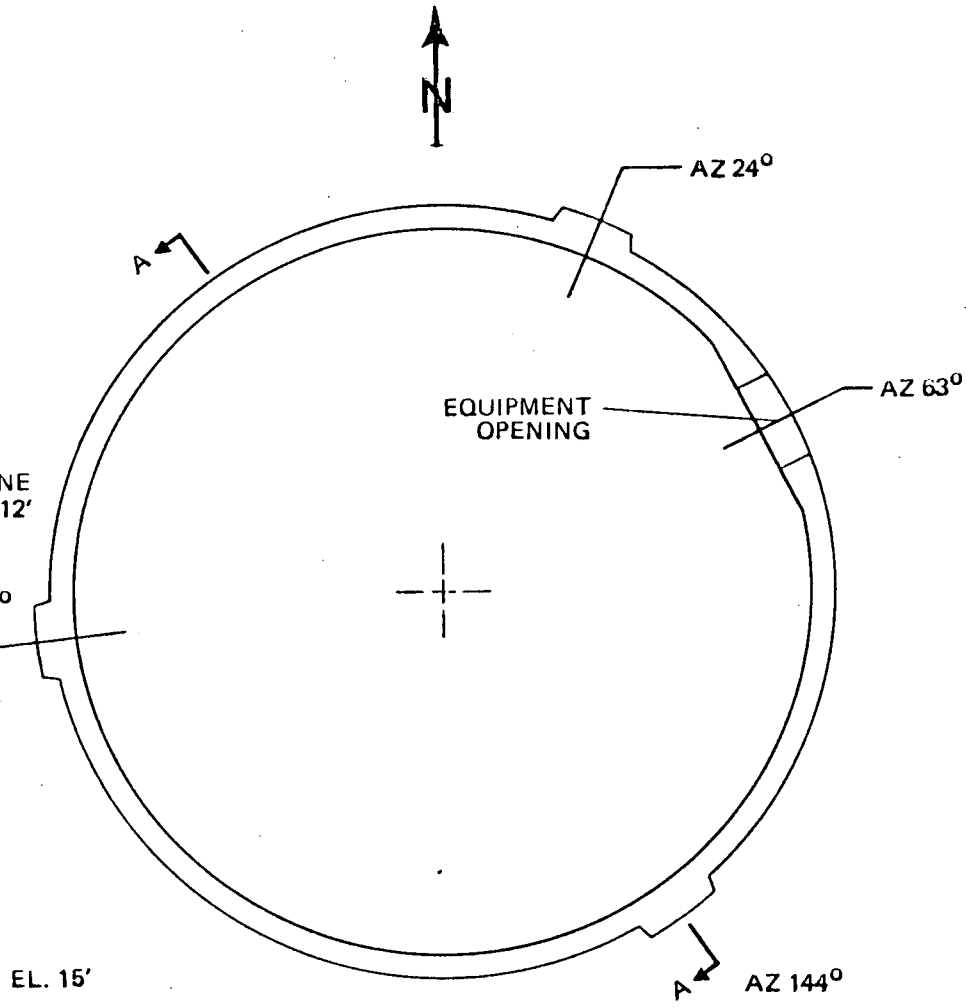

PLAN SECTION THROUGH
CONTAINMENT AT EQUIPMENT
OPENING ℄ ELEVATION (EL. 38)

FIGURE 3.1 - CONTAINMENT STRUCTURE

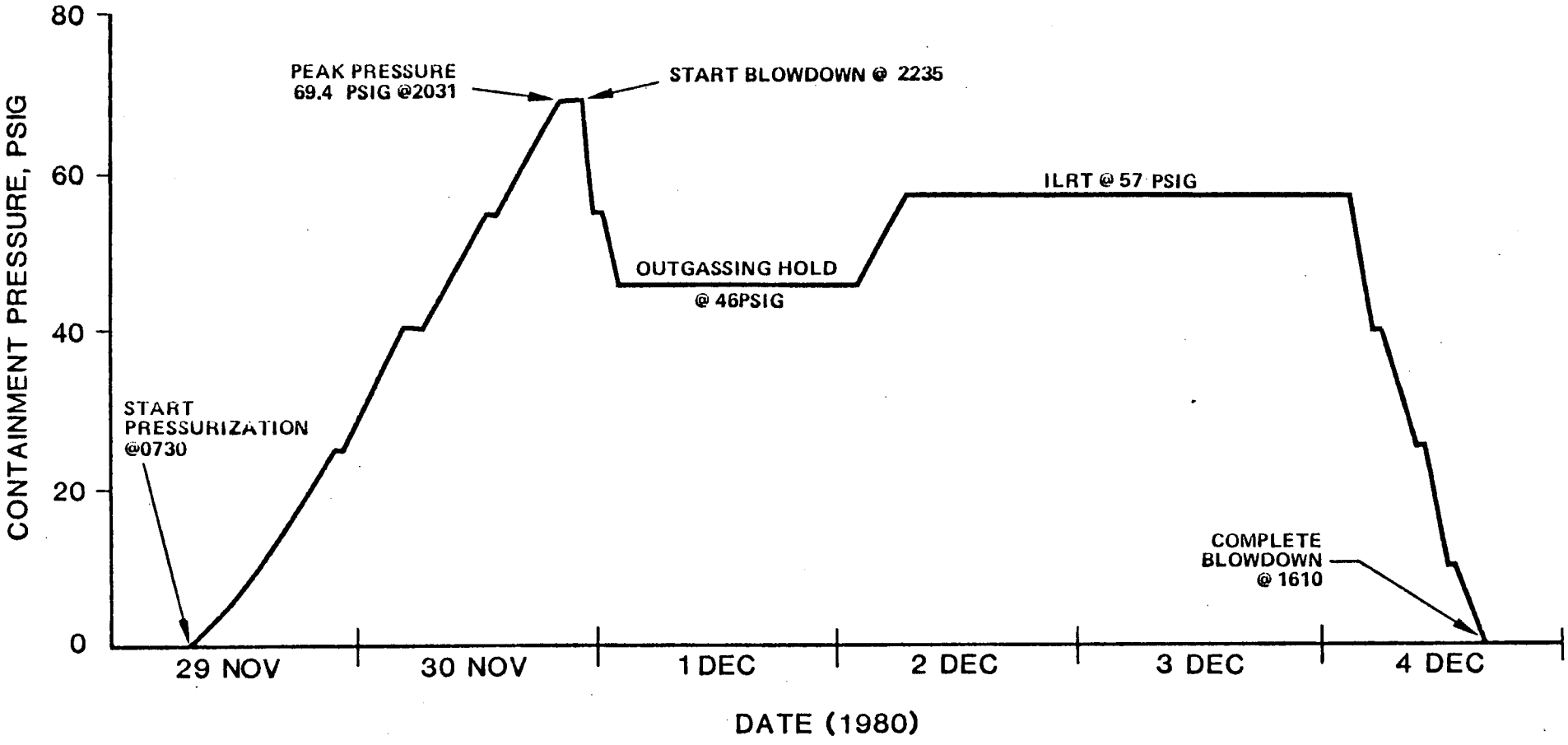

FIGURE 3.2 - CONTAINMENT PRESSURE CYCLE

4. TEST PLAN AND PROCEDURES

To accomplish the objectives of the structural integrity test, the containment was pressurized to 1.15 times design pressure and then depressurized, with various intermediate pressure cycles and plateaus as needed to acquire structural test data and to satisfy the requirements of the concurrently conducted integrated leakage rate test. Pressurization to 1.15 times design pressure was specified to demonstrate that the containment has a margin of safety with respect to the internal pressure loading. Containment response to internal pressure was measured in order to verify that the analytical techniques used in the design can accurately define the behavior of the structural elements. The details of the structural response measurements - deformation, strain and surface crack growth - are described below.

4.1 Deformation Measurements

Radial and vertical movements of the containment shell were measured at the points shown in Figures 4.1 through 4.3. The indicated points are on regular areas of the containment shell as well as on the discontinuity regions represented by a buttress and the equipment opening. Movements were measured by taut wire extensometers attached to one point on the shell and spanning to an opposing point on the shell or to a point on the interior structure.

The extensometer utilizes an Invar wire to actuate a linear variable differential transformer which in turn generates an electrical signal proportional to containment movement. The .05 inch diameter wire is attached at one end to a fixture mounted on the shell liner or on the interior structure and at the opposite end to the core shaft of the transformer. The annular coil element of the transformer is mounted in a cylindrical housing which is, in turn, rigidly fixed to the containment liner or to the interior structure. The housing contains a coil spring which maintains a pull of approximately 20 lb. on the transformer core shaft and the wire. Relative movement between the points to which the wire and housing are attached is transmitted through the wire and results in an almost equal relative movement between the core shaft and coil element of the transformer. This movement between core and coil changes the electrical output of the transformer by a proportional amount. The electrical signal is recorded - cable from the transformer is fed through an electrical penetration to a data acquisition system - and converted, using appropriate calibration constants, to containment movement. The extensometers are calibrated in a test jig to establish the transformer displacement/output relationship, the displacement/spring force relationship and the friction forces which cause a dead band when the direction of movement of the core changes. Containment movements are calculated as the product of transformer output voltage change, the displacement/output voltage ratio and the spring force correction factor. This last factor corrects for changes in Invar wire length due to the displacement induced changes in spring force. The extensometer assembly is relatively insensitive to changes in temperature over the range encountered during the structural integrity test.

The final adjustment of core position in the installed extensometer is made by extending the core (using a turnbuckle) in the direction of movement

anticipated during presurization. This is done to insure that there is no deadband in extensometer response during initial pressurization to test pressure. During subsequent pressure cycles the deadband effects can be noticed (as discussed in Section 5) in the test data. The displacement error due to deadband is the product of the wire spring constant (L/AE) and the friction force in the transformer core suspension.

Extensometer attachment fittings on the containment liner are installed close to or directly over line stiffeners to insure that the measured movement represents only concrete displacement and does not reflect the closing and opening of small gaps between the 1/4 in. liner plate and the concrete.

4.2 Strain Measurements

The hoop and meridional components of concrete strain were measured at the locations shown in Figure 4.4. At each location, the two strain componnents were measured at the inner curtain of reinforcing steel, at the midthickness of the concrete, and at the outer curtain of reinforcing steel.

Concrete strain is sensed by resistance strain gages bonded to a short length of No. 4 reinforcing bar embedded in the structure. The strain gages are shop mounted to flats milled at the center of the bar and covered with epoxy layers and heat shrinkable tubing for protection against moisture intrusion and mechanical damage. The milling reduces the bar cross section by about 5% and increases the strain at the gage location by approximately the same factor. Each end of the bar terminates in a hook. The outside to outside of hook length is 3.5 ft. The true gage length (the length over which strain is averaged) depends on the exact nature of the bond between the No. 4 bar and the concrete and is not definitely known. Over the regular areas of the cylinder and dome strain gradients are small and the uncertainty in gage length does not influence the interpretation of measured strain. However, in discontinuity regions where strain gradient is high, the uncertainty is reflected as a discrepancy between the measured strain and the value calculated for the location of the bar center.

The bars were attached to the normal reinforcing steel, or to auxiliary bars, during containment construction. The signal cables wired to the strain gages were tied to reinforcing steel between the instrumented bars and the ends of embedded conduit and were pulled through the conduit to junction boxes opening at the exterior surface of the concrete. Following the completion of containment concrete placement the signal cables were extended from these junction boxes to a data recording device.

Concrete temperatures were measured at each strain sensor location to provide the data needed for evaluating the thermal component of total strain. The construction of the strain sensors is such that the indicated strain is the sum of mechanical strain and strain due to thermal stress.

Unrestrained thermal expansion is sensed only as a differential between concrete and steel - a small amount.

Temperature is sensed by a linearized thermistor network embedded in the strain gage expoxy covering. The thermistor network is wired to additional conductors in the strain gage signal cable and connected to the data recording system.

4.3 Concrete Surface Surveillance

Concrete surface cracking was monitored in seven areas as shown on Figure 4.5. Each area covered 40 or more square feet and was divided into one foot squares by snapped-on chalk lines. The areas were examined for surface cracks per the schedule in Subsection 4.5. Each observed crack was measured using a 30 power magnifier with an etched scale in the optical system. Cracks which were .01 inches or more in width were detailed on data sheets.

4.4 Other Measurements

Containment gage pressure was measured by a calibrated ($\pm$0.1 psig) bourdon tube gage. In containment temperature and humidity were recorded by the leakage rate test data acquisition equipment. Outside ambient conditions were measured using a sling psychrometer and a bourdon tube barometer (absolute pressure gage).

4.5 Data Acquisition

Deformation, strain and concrete temperature data were printed on paper tape by a digital data acquisition system. The printer also recorded date and time. Each tape was manually annotated with containment gage pressure, barometric pressure and outside ambient dry and wetbulb temperatures. Tapes were generated at 5 psig containment pressure increments/decrements, at the beginning and end of all pressure plateaus and at regular intervals prior to pressurization, during plateaus and following depressurization per Reference a.

Concrete surface crack inspections were performed prior to the start of pressurization, at 40 psig during initial pressurization, at peak test pressure and following the completion of final blowdown.

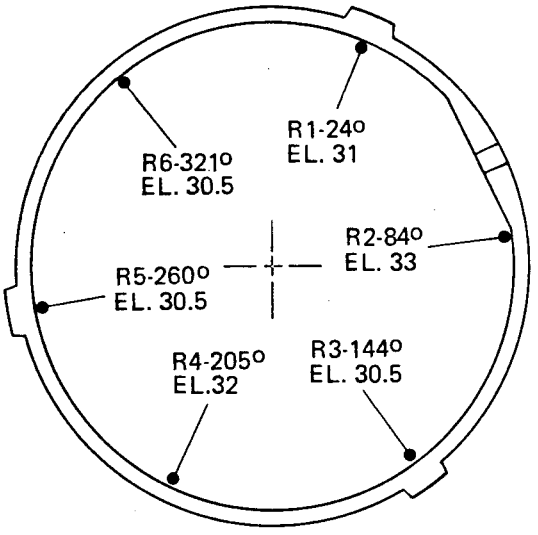

PLAN @ EL. 30±

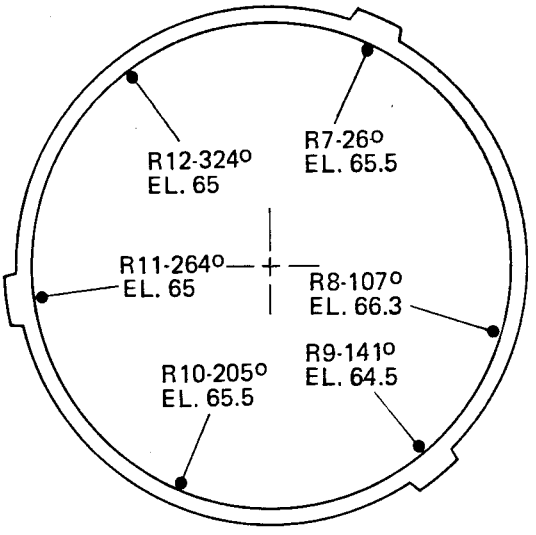

PLAN @ EL. 65±

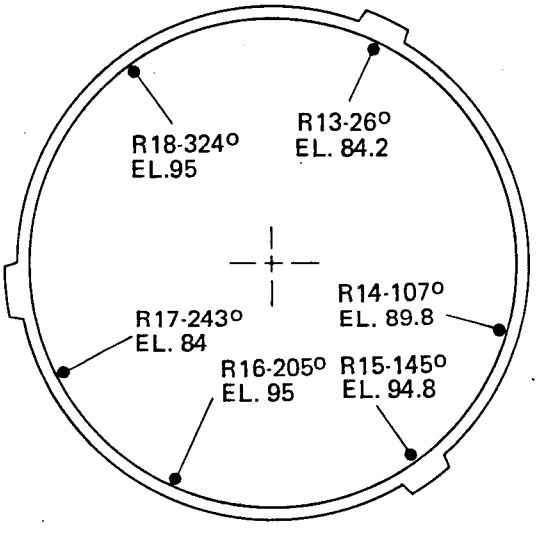

PLAN @ EL. 90±

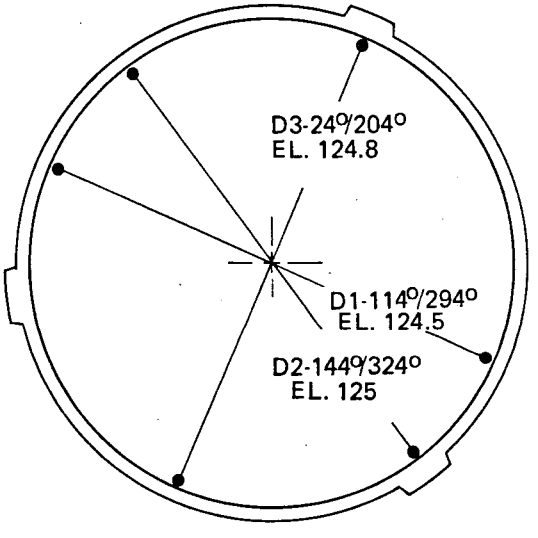

PLAN @ EL. 125±

FIGURE 4.1 TAUT WIRE EXTENSOMETER LOCATIONS WALL RADIAL/DIAMETRAL UNITS

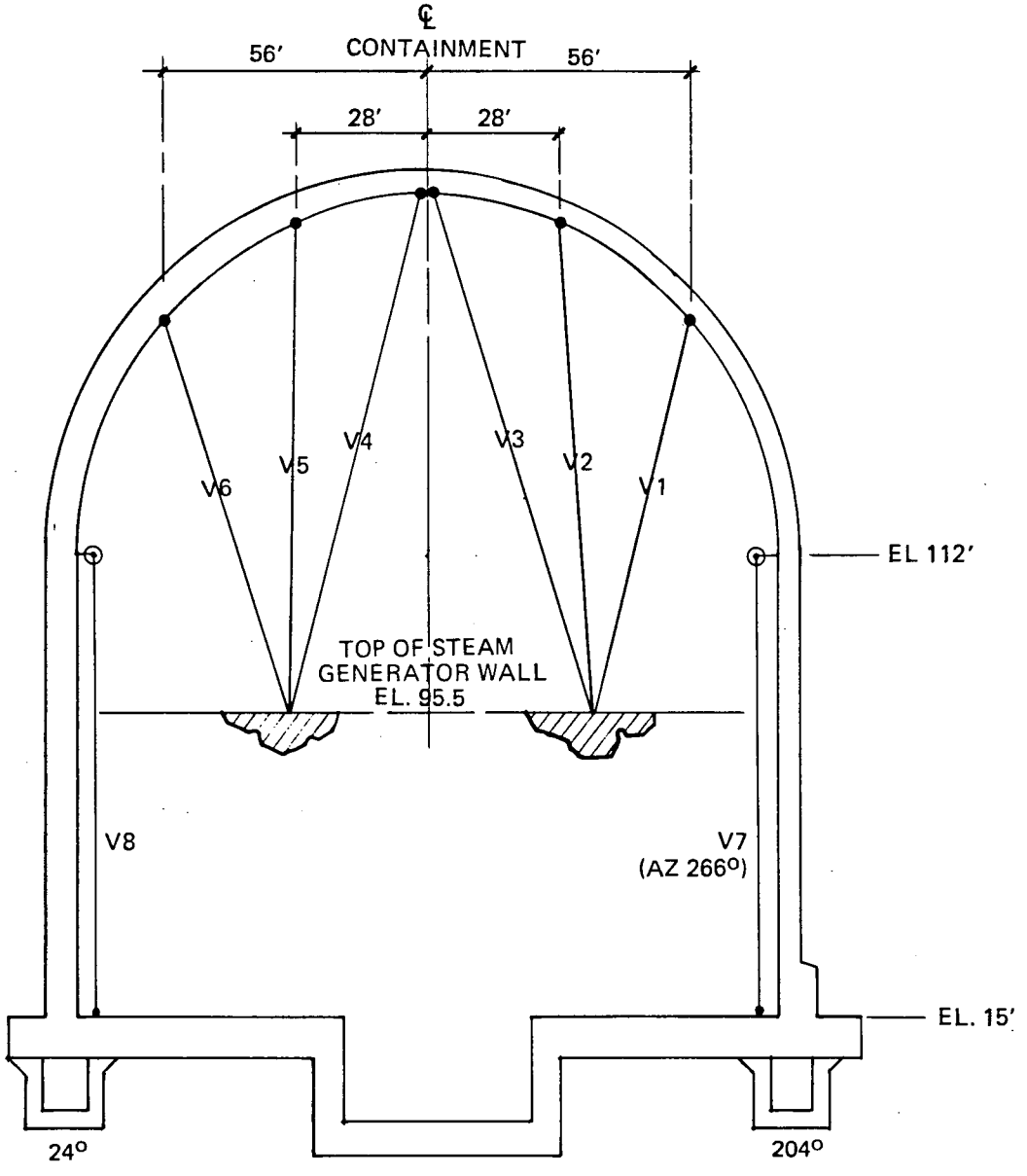

ELEVATION SECTION THROUGH CONTAINMENT & 24°/ 204°

FIGURE 4.2 - TAUT WIRE EXTENSOMETER LOCATIONS VERTICAL UNITS

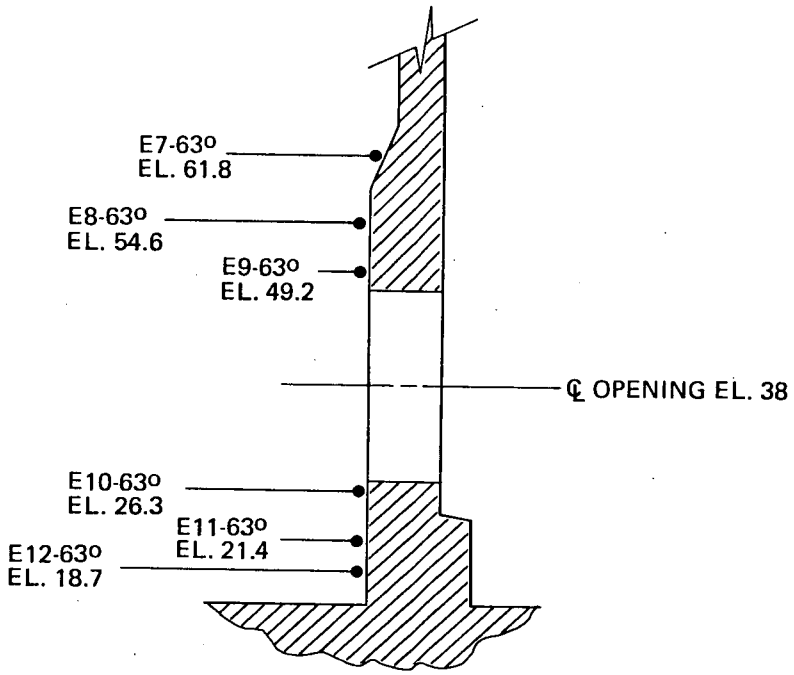

ELEVATION SECTION THROUGH
EQUIPMENT OPENING ℄ @ 63°

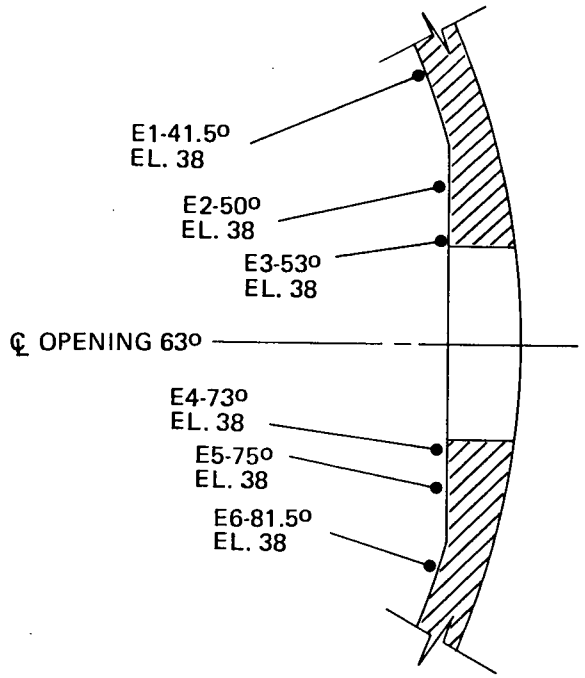

PLAN SECTION THROUGH
EQUIPMENT OPENING ℄ @ EL. 38

FIGURE 4.3 TAUT WIRE EXTENSUMETER LOCATIONS EQUIPMENT OPENING UNITS

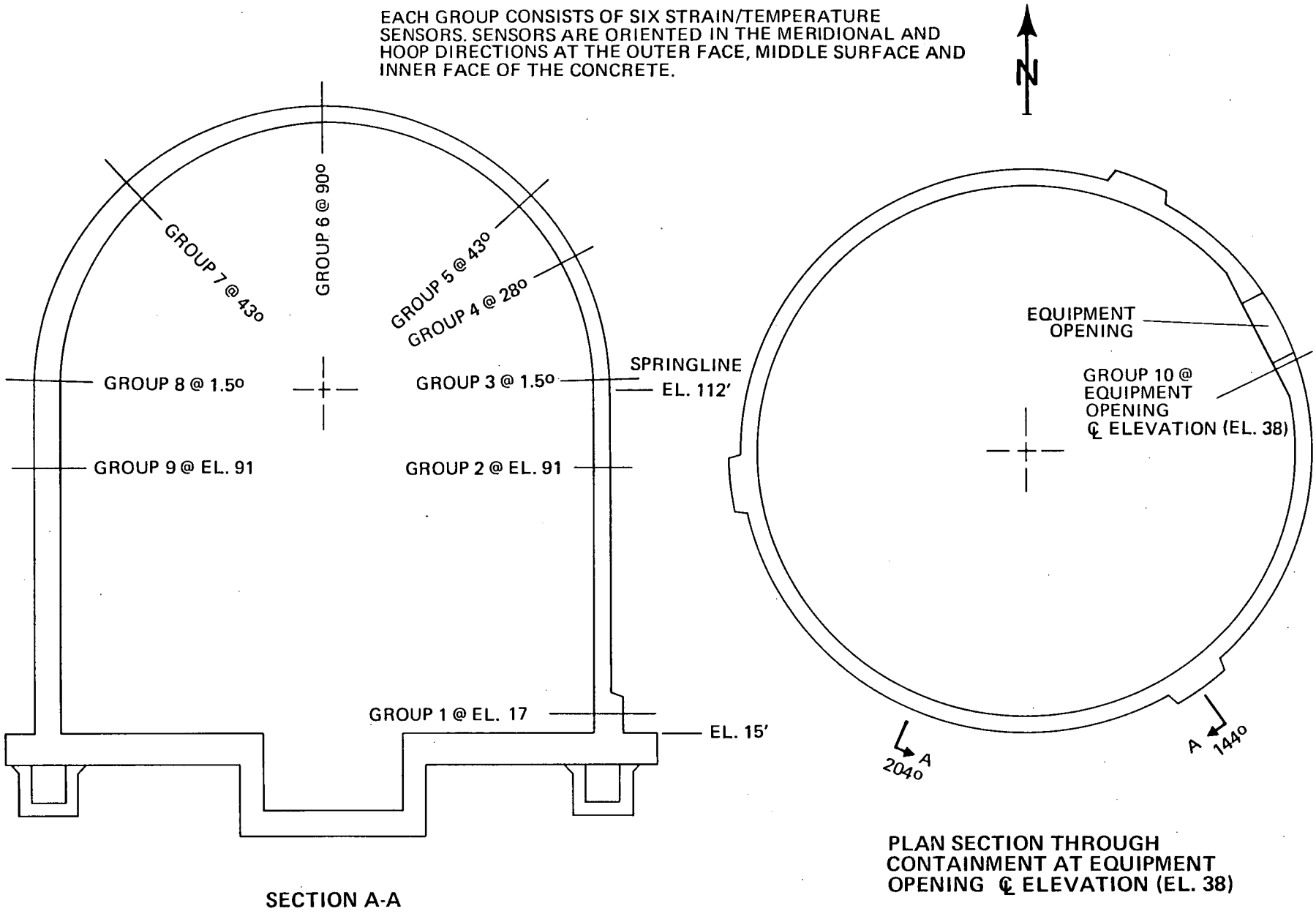

FIGURE 4.4 - STRAIN SENSOR LOCATIONS

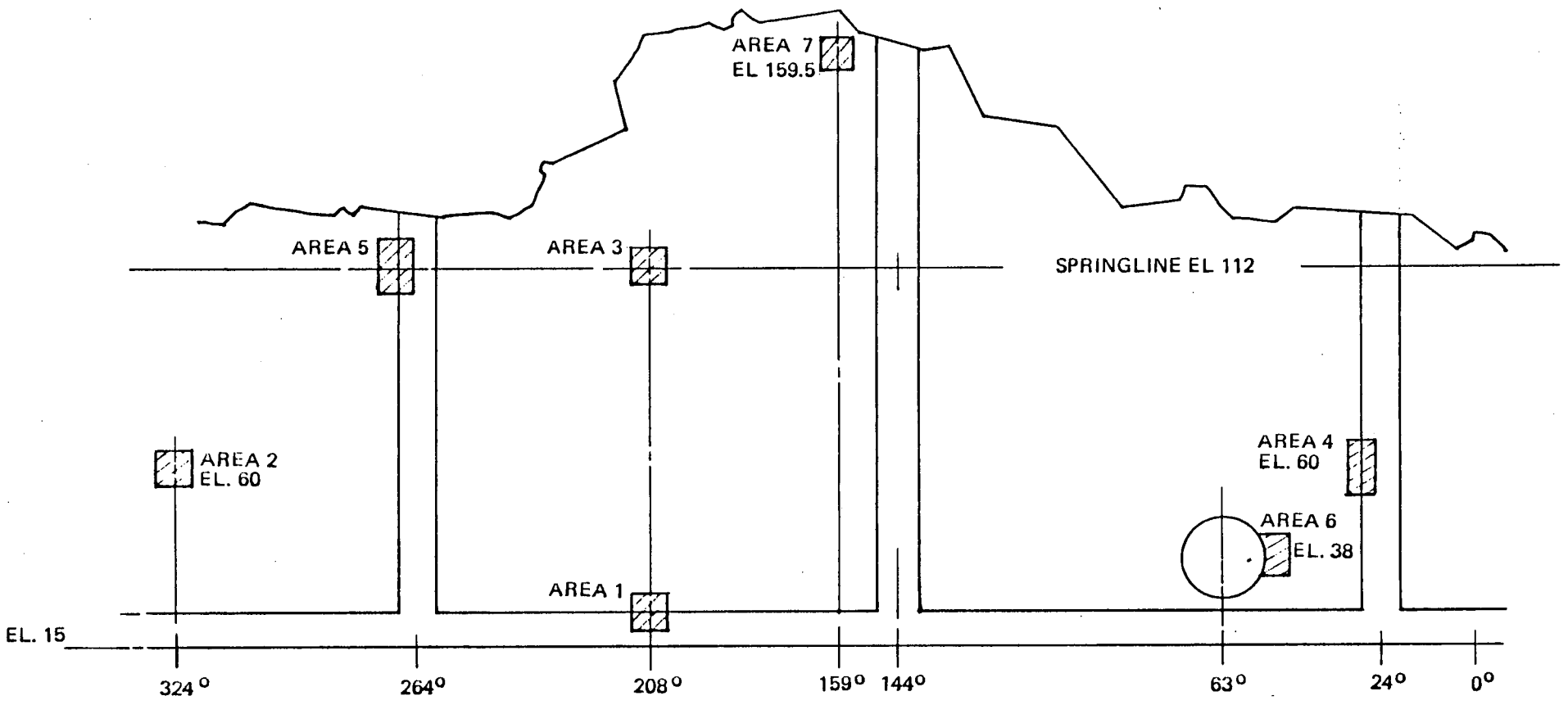

DEVELOPED ELEVATION OF CONTAINMENT

FIGURE - 4.5 CONCRETE SURFACE SURVEILLANCE AREAS

5. TEST RESULTS

5.1 Containment Deformations

Containment shell movements at peak test pressure (69.4 psig) were close to predicted values as shown in Figure 5.1. The measured values shown on the figure represent the mean of all movements measured at the specified elevations. On the cylinder wall the individual radial movements measured at each elevation varied from point to point but were quite consistent across the three instrumented diameters. Table 5.1 below lists the individual radial movements, the average radial movements across the instrumented diameters, the mean of all radial movements at each elevation and the predicted values of these movements.

Elevation 31		Elevation 65		Elevation 90		Elevation 125	
Azimuth	Movement	Azimuth	Movement	Azimuth	Movement	Azimuth	Movement
24° B	.099 in.	26° B	.175 in.	26° B	.210 in.	114°/294° WW	.127 in.
205° W	.183	205° W	.274	205° W	.306	144°/324° BW	*
24/205A	.141	26/205 A	.224	26/205 A	.258	24°/204° BW	.115
84 ° W	.193	107° W	.392	107° W	.408		
260° B	.077	264° B	.098	243° B	.128		
84/260A	.135	107/264 A	.245	107/243 A	.268		
144° B	.096	141° B	.234	145° B	.282		
321° W	.123	324° W	.207	324° W	.230		
144/321A	.110	141/324 A	.220	145/324 A	.256		
MEAN	.128		.230		.261		.121
PREDICTED	. 11		.22		.22		.13

W - Wall Section B - Buttress Section A - Average Radial Movement of Opposite Wall/Buttress Points

* Sensor Malfunctioned

TABLE 5.1 WALL RADIAL MOVEMENTS AT 69.4 PSIG

At the lowest elevation (El. 31) where wall bending is most significant, the variation is seen to be almost entirely due to the stiffening effect of the buttresses. The buttress effect is still apparent at the 65 and 90 ft. elevations but roundout of the single curvature cylinder wall, as well as interior structure

datum displacement contributes to the variation. This roundout is normal for containment structures, all of which deviate slightly from a perfectly circular shape. The extensometers at elevations 31, 65, and 90 are connected to datum points on the interior structure which rests on the containment base mat. Therefore, any slight tendancy of this structure to rotate as a result of mat bowing will be reflected as variations in radial measurements of wall movement. Thus, the measured values listed in Table 5. 1 and shown in Figure 5.1 probably exceed true wall movements by a small amount.

At El. 125 on the spherical dome the two full diameter extensometers show essentially the same movement. This is expected since the full diameter measurements are not affected by displacements of the interior structure and since the double curvature sphere is less susceptible to roundout under load than is the single curvature cylinder wall.

Individual vertical movements of the wall and dome are listed in Table 5.2 below. Predicted values for both flexible (as modelled) and rigid base mat assumptions are included in the Table.

Wall Azimuth	Vertical Movement	Dome at R = 56' Azimuth	Dome at R = 56' Movement	Dome at R = 28' Azimuth	Dome at R = 28' Movement	Dome at Apex Azimuth	Dome at Apex Movement
266° B	.096	204° W	.313	204° W	.394	204° W	.388
26° B	.096	24° B	.247	24° B	.366	24° B	.386
Predicted	.096		.56/.25*		.66/.35*		.67/.36*

W - Wall Section B - Buttress Section

* First Figure - Flexible Mat; Second Figure - Rigid Mat

TABLE 5.2 VERTICAL MOVEMENTS AT 69.4 PSIG

Both extensometers measuring vertical movements of the wall between the base mat and springline show the same movement. This is expected since the vertical elongation of the wall is not influenced by local bending and roundout. While both units are located at buttress sections, regular wall sections should show about the same movement since earlier structural integrity tests have demonstrated that shear lag in containment walls is negligible.

The vertical movements of the dome show that the buttress stiffening effect decreases with increasing distance from the springline. At the 56 ft. radius (distance from containment centerline) the buttress section moved upward only 79% as much as the regular spherical section. At the 28 ft. radius, the corresponding figure is 93%. At the apex, the movements are the same as

expected. This illustrates that the steam generator walls to which the extensometers are attached moved (with the base mat) equally. All six vertical movements of the dome are referenced to the tops of the steam generator walls. Since these walls will move downward with the base mat, the measured values of dome movement are probably greater than actual values and, thus, conservatively reported. The predicted dome movement illustrated by the dashed line in Figure 5.1 is movement referenced to the wall/base mat juncture.

The measured vertical and diametral deformations at the points of maximum predicted deformation were less than the acceptance limit of 125% of predicted values.

The radial movements measured near the equipment opening are illustrated in Figure 5.2. The measurements on the horizontal plane at El. 38 indicate that there is relatively little variation in outward movement with distance from the edge of the opening and, thus, relatively, little bending of the thickened section about a vertical axis. Since the opening is not symmetrically located with respect to the buttresses, the side of the opening adjacent to the buttress at 24° moves less than the opposite side, as expected.

The measurements in the vertical plane at 63° (opening centerline) show that outward movement increases rapidly with increasing distance from the basemat juncture to the top of the opening. Above the opening there is no distinct trend since the movement appears to be independent of distance from the top of the opening. The measured outward movement at El. 61.8 is .310 inches which is between the .175 inch and .392 inch movements, measured at El. 65 and 26° (buttress) and 107° (wall), respectively. The movements above the opening are thus consistent with the values expected on the basis of the measured movements of the cylinder a reasonable distance away.

The variation of deformation with pressure is illustrated in Figures 5.3 through 5.5. The deformation/pressure relationships are reasonably linear. Following the end of the peak pressure hold period the deformation/pressure relationships show an offset, or dead band, effect. This effect is caused by small friction forces in the differential transformer core suspension which change the length of the Invar wire as the direction of movement reverses. The offset is most apparent in the differences between measured movements at the 55 psig plateaus before and following the peak pressure hold period. The maximum offsets are on the order of .05 inches. An offset is also apparent at the completion of final blowdown. This offset is a combination of extensometer dead band and incomplete recovery of the delayed elastic strain in the containment concrete. The delayed elastic response is covered in Subsection 5.2 below.

5.2 Concrete Strains

Measured concrete strains along a typical wall section at peak test pressure (69.4 psig) were generally close to predicted values as listed in Table 5.3 below.

SENSOR LOCATION & DIRECTION		STRAIN, MICROINCHES/INCH					
Elevation or Vertical Azimuth (Dome)	Direction	Inside Face of Concrete		Middle Surface of Concrete		Outside Surface of Concrete	
		Predicted	Measured	Predicted	Measured	Predicted	Measured
El. 17	Meridian	200	289	61	77	-110	-126
El. 17	Hoop	33	4	39	-11	39	19
El. 91	Meridian	66	77	72	106	84	112
El. 91	Hoop	234	246	231	205	224	255
El. 12	Meridian	90	119	93	129	93	106
El. 112	Hoop	179	166	177	134	173	154
Az. 28°	Meridian	121	133	117	101	110	97
Az. 28°	Hoop	113	122	112	112	107	112
Az. 43°	Meridian	119	110	117	126	114	91
Az. 43°	Hoop	116	105	114	118	111	88
Apex	Meridian	119	99	116	113	113	127
Apex	Hoop	119	94	117	114	113	131

TABLE 5.3

PREDICTED AND MEASURED CONCRETE STRAINS ON 204° CONTAINMENT AZIMUTH AT 69 PSIG

The largest differences between measurements and predictions are at the wall/base mat juncture where strain gradients are high. As discussed in Subsection 4.2, the uncertainties in the true gage lengths and the exact positions of the sensors can be expected to result in relatively large discrepancies between measurements and predictions in zones of high strain gradient.

At the remaining locations covered in Table 5.3 the differences between measurements and predictions are smaller and tend to be more or less randomly distributed between positive and negative values. The differences result from several factors, principal among which are:

- The strain sensors, due to the design (per Subsection 4.2), indicate a strain somewhat larger than actual.

- The actual material properties of the concrete will differ somewhat from those used in the analysis.

- Changing thermal gradients in the concrete cause non-uniform variations in the thermal component of strain.

- The strain gradient effect discussed above is active to some degree at all points on the structure.

- The anlysis does not include the buttress stiffening effect which is present to some degree at all points on the structure.

Confidence in the aggregate precision of the sensors (the ability of all sensors to respond equally to imposed strain) is demonstrated by the measurements at the dome apex. At the apex, hoop and meridional strain are the same (except for minor discontinuity effects caused by the buttresses) due to symmetry. The three sensor pairs at the apex indicate equal ($\pm$ 5 microinches/inch) hoop and meridional strains as expected.

Strains measured at the edge of the equipment opening are shown in Figure 5.6. The expected trends are apparent, as follows: tangential strains are larger than radial strains; strains increase from inside to outside; and strain magnitudes in the thickened section are similar to those in the unthickened, but continuous, wall.

Typical strain/pressure time histories are shown in figures 5.7 through 5.10. Strains at most sensor locations are linear with pressure until the final rapid depressurization of the containment. The non-linerity is reflected in the residual strain at zero pressure which results from the slow strain increase (delayed elastic response) in the concrete during the 90 ($\pm$) hours of sustained pressure load.

The strain at the outside edge of the equipment opening (Figure 5.10) shows a non-linear strain/pressure relationship during initial pressurization. This non-linearity is probably the result of predicted minor cracking of the concrete at this point. The increase in strain during the integrated leakage rate test plateau at 57 psig may result from slow crack development during the sustained high pressure load.

Figure 5.11 illustrates an extreme temperature gradient effect. Due to positioning tolerances, this sensor probably has a minimum of concrete cover and is subjct to higher than normal temperature changes induced by outside ambient conditions. The dashed line on the plot represents as recorded strains. Recorded temperatures are noted at the inflection points on the plot. The solid line represents strains corrected for temperature change

using a thermal expansion coefficient of 6 X 10-6/°F and is reasonably linear with pressure. This plot demonstrates the potential magnitude of the temperature gradient effect and serves to explain one source of the measurement/prediction differences noted in Table 5.3.

5.3 Concrete Surface Surveillance

Figures 5.12 through 5.18 show the concrete surface cracking data recorded during the structural integrity test. All cracks lying within the observation areas and having widths equal to or greater than .01 inches were examined and sketched at each stage per Subsection 4.5. Increases in crack widths at peak test pressure were generally less than .01 inches. The largest recorded crack width increase, in Area 7 on the dome (Figure 5-18), was .035 in. which is well below the acceptance limit of .060 in. During the structural integrity test crack widths were measured directly at the surface of the concrete which is appropriate for determining width increase. The true widths of the cracks just below the concrete surface are generally less.

5.4 Estimated Accuracy of Measurement

Deformation Measurements

The differential transformers in the extensometers are calibrated to a repeatability of .001 inches. Measurement errors in the assembled extensometers are introduced by temperature changes and friction forces. The effect of temperature is small. The maximum friction force in the transformer core suspension is on the order of .15 lb if the extensometer housing is properly aligned with the Invar wire. Reversing the dirction of core movement results in a change in wire force of 0.3 lb which causes a measurement error proportional to wire length. The following table lists maximum error for wires of 25, 50, --150 ft.

Length, Ft.	25	50	75	100	125	150
Error, In.	.002	.003	.005	.006	.008	.009

If the extensometer housing is misaligned due to careless installation or later tampering, the friction forces can be much higher than .15 lb and the error will increase accordingly.

The transformer output is sensitive to excitation voltage and over some reasonable range, varies linearly with excitation. Actual excitation at any extensometer will vary by as much as 0.1 volts from the calibration excitation of 24.00 V giving an error of less than $\pm$ 0.5% of measured displacement. This represents a maximum measurement error of .002 in at the maximum displacement of 0.4 inches.

Summing the extreme errors listed above (assuming a properly installed extensometer) gives a maximum measurement error of .012 inches.

Strain Measurements

The sensors used to measure strain develop bond in the concrete over a finite length. Thus, in regions of high strain gradient the measured strain will not correspond to the strain at the point where the center section of the sensor is located. The difference between measured strain and strain at the center point depends on the strain gradient and bonding characteristics and cannot be evaluated analytically. Therefore, no accuracy estimates are given for gradient error.

The center section of the sensors is milled to provide a bonding surface for the strain gages. Milling removes approximately 5% of the steel cross section and results in the strain at this section being about 5% greater than strain in the adjacent full sections. The resulting measurement error is systematic and can be corrected. The nominal correction factor of .95 is not exact since the milling process can leave more or less metal at the instrumented section. The range of net reduction in section probably varies from 4% to 7%.

Variation in strain gage resistance, gage factor and transverse sensitivity and in lead cable resistance probably introduce an uncertaintly of about $\pm$3% into the strain measurement.

Measurement error at the data acquisition system is, based on observation, not greater than $\pm$3 microinches per inch. Errors introduced by spurious voltages impressed on the signal cables can be much larger. However, there was no indication that this common mode error exceeded $\pm$10 microinches/inch during the test.

Applying the worst combination of the above errors results in a gross uncertainty in strain measurement of 5%$\pm$10 microinches/inch not including the nominal 5% error caused by sensor milling.

The thermistor networks embedded in the strain sensors respond to temperature change (over the range encountered during the test) to better than 0.5F.

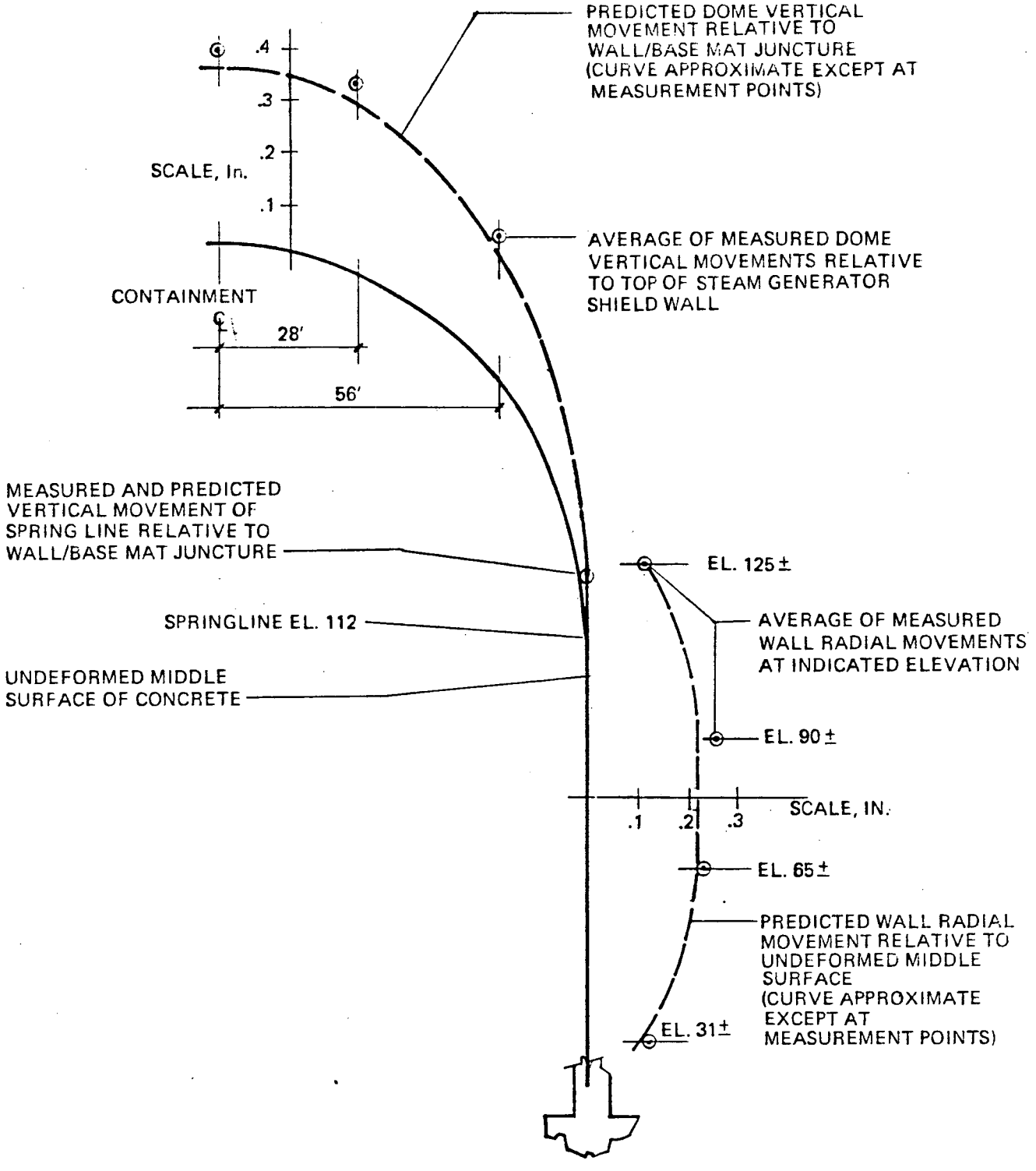

FIGURE 5.1 - CONTAINMENT DEFORMATIONS AT 69.4 PSIG WALL & DOME

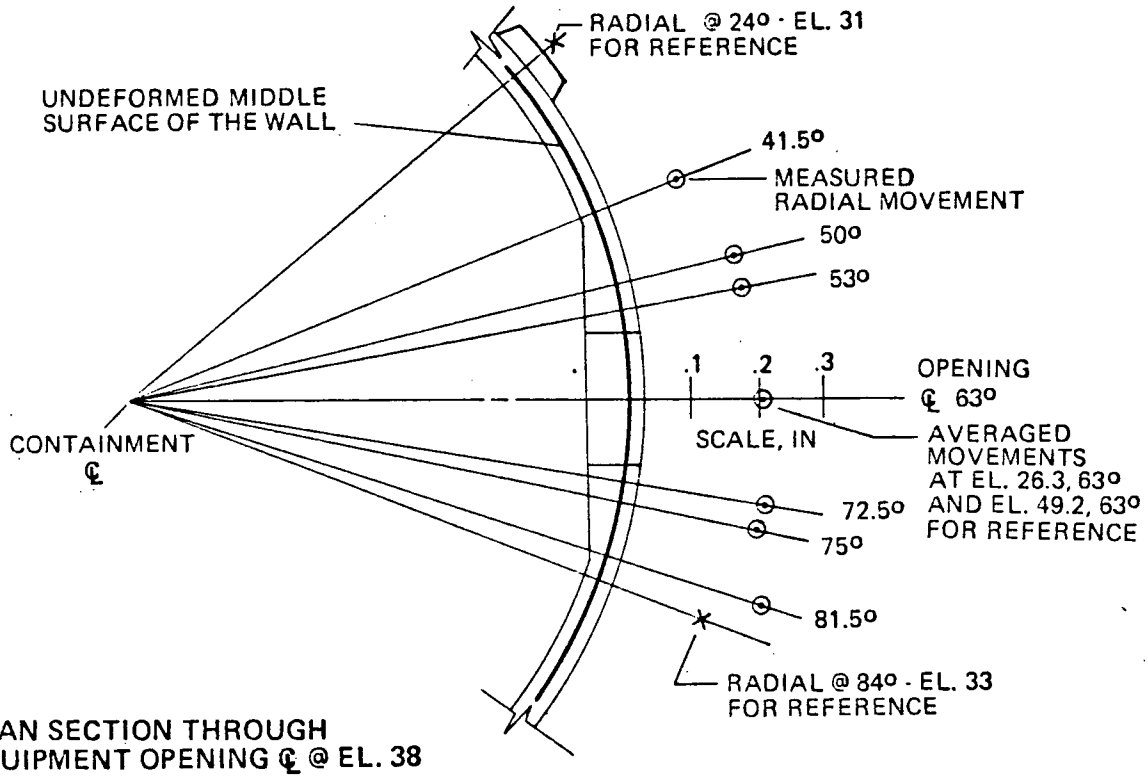

PLAN SECTION THROUGH
EQUIPMENT OPENING ℄ @ EL. 38

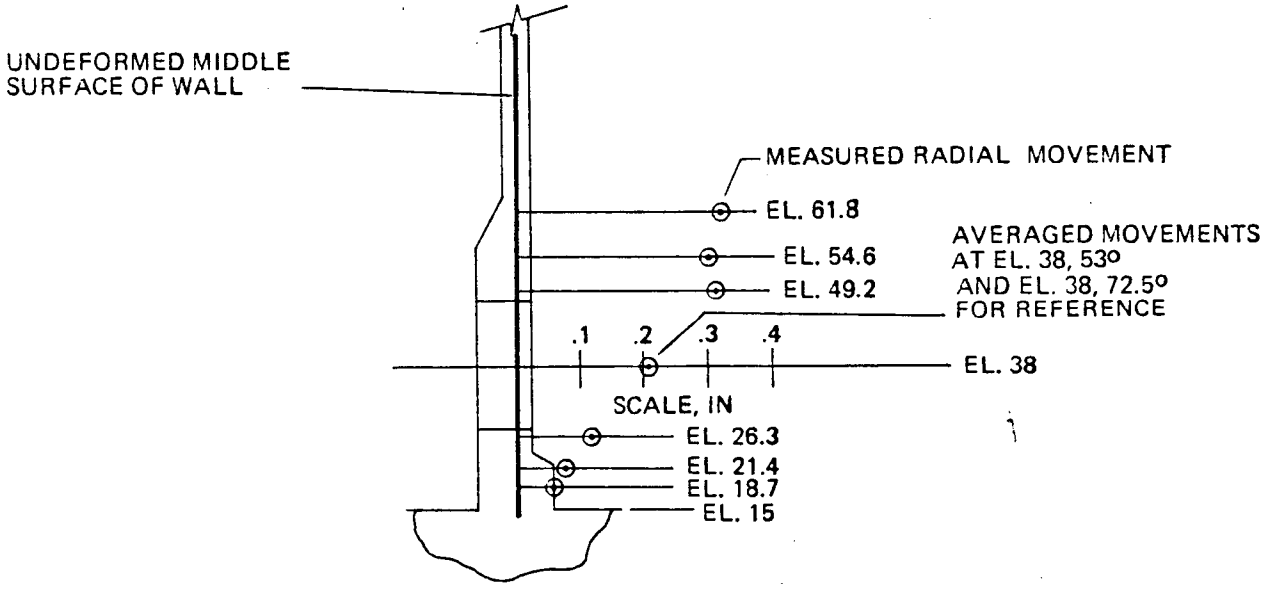

ELEVATION SECTION THROUGH
EQUIPMENT OPENING ℄ @ 63°

FIGURE 5.2 CONTAINMENT DEFORMATIONS AT 69.4 PSIG EQUIPMENT OPENING

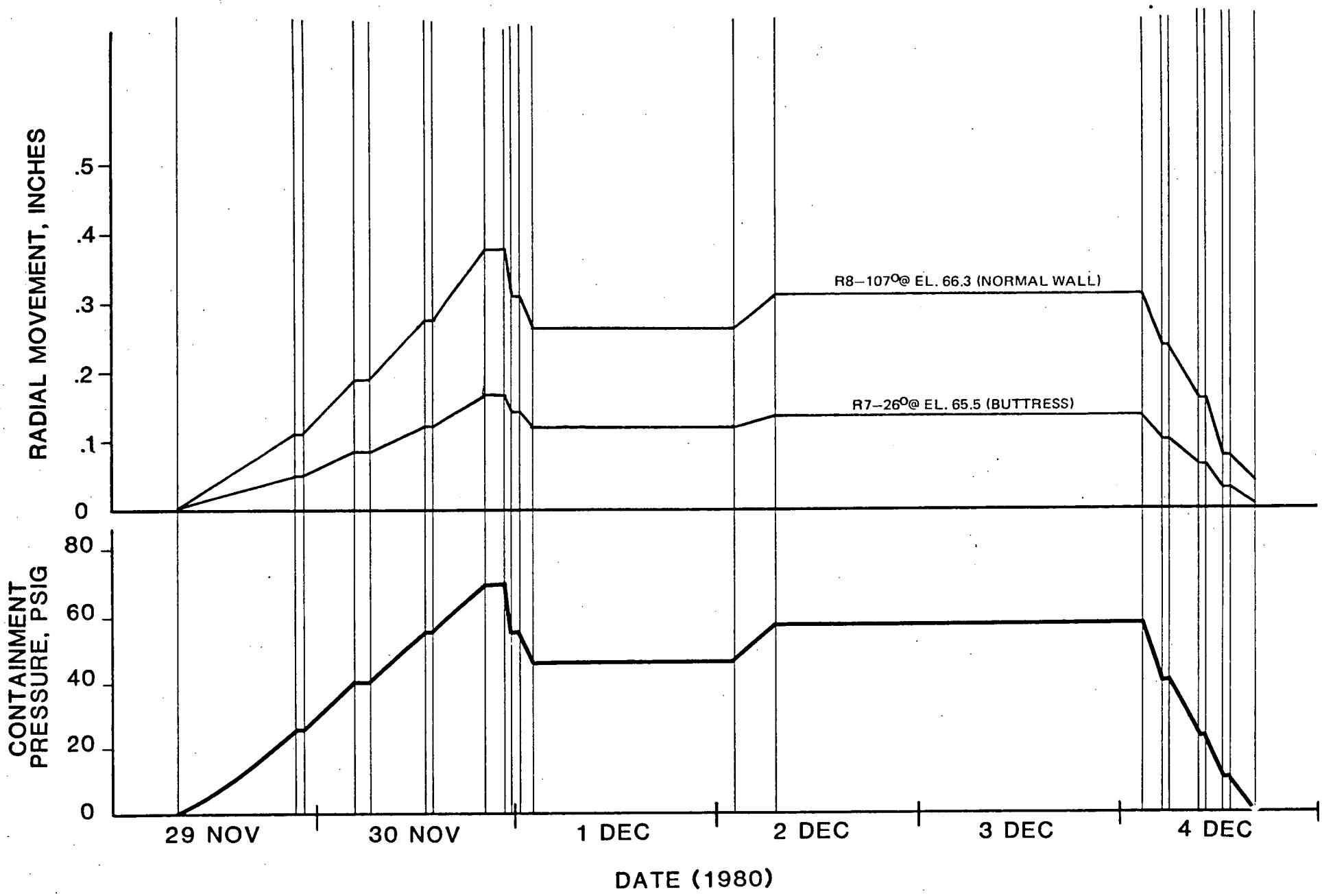

FIGURE 5.3 - TYPICAL DEFORMATION/PRESSURE TIME HISTORY WALL/BUTTRESS RADIAL MOVEMENT

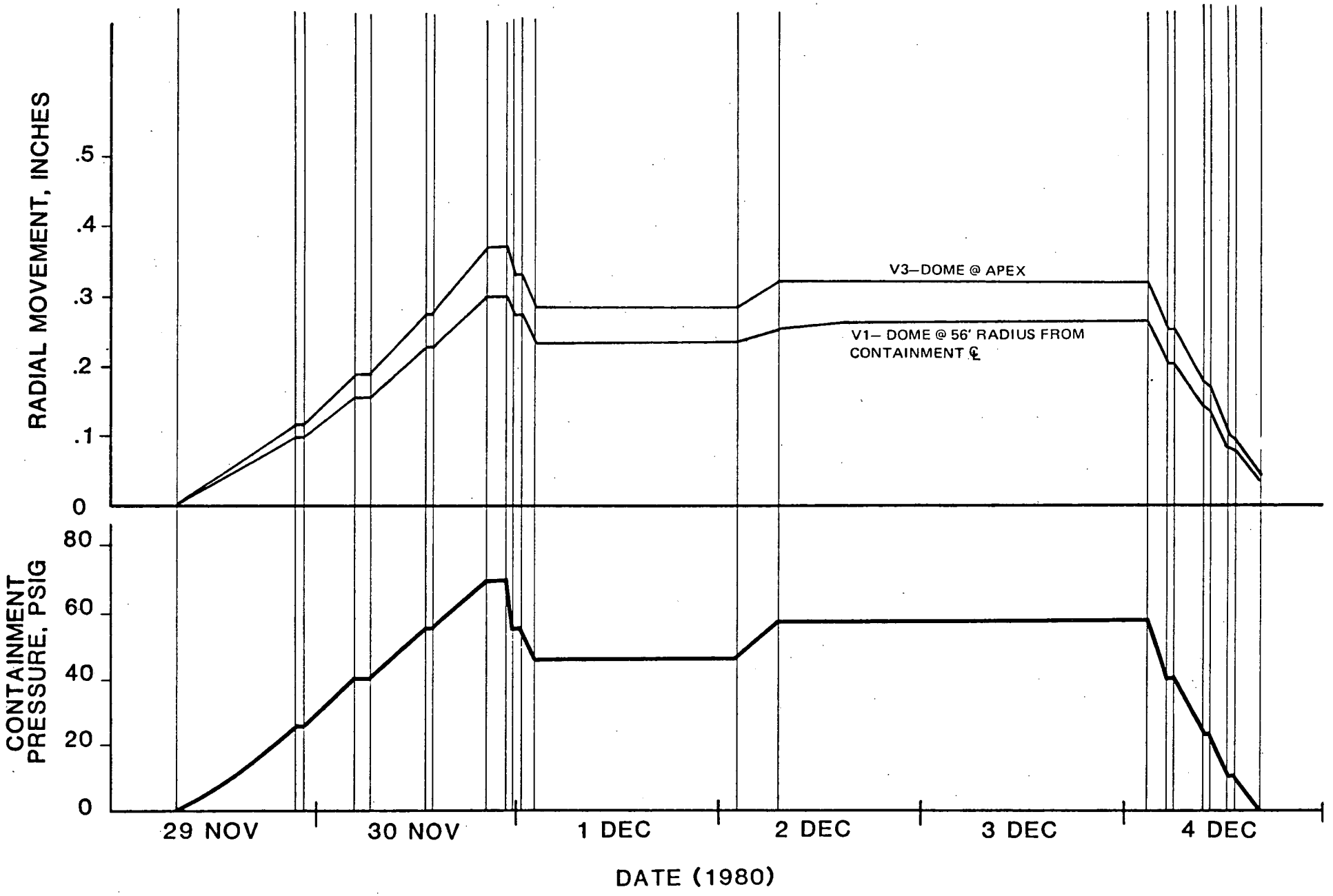

FIGURE 5.4 - TYPICAL DEFORMATION /PRESSURE TIME HISTORY DOME VERTICAL MOVEMENT

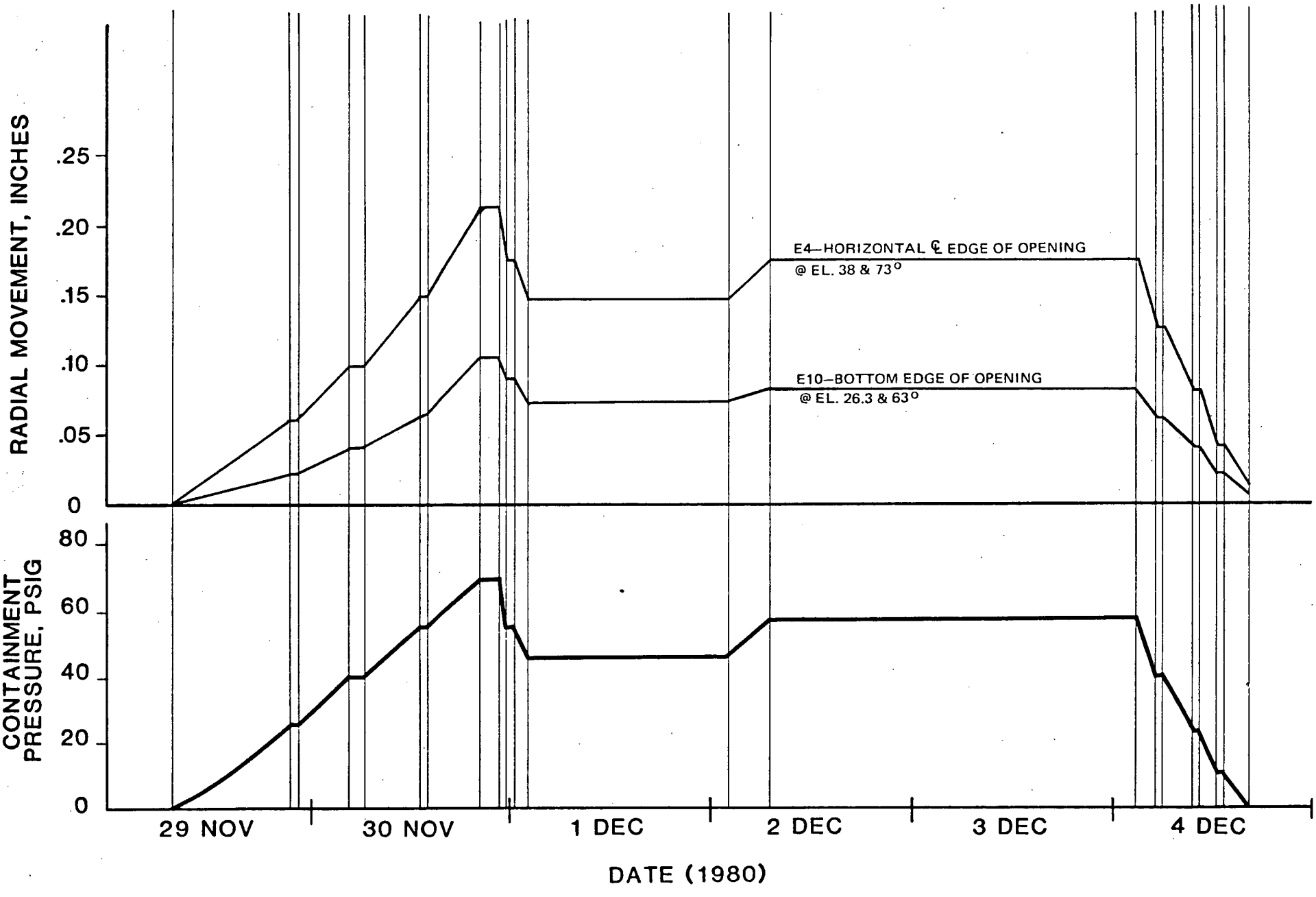

FIGURE 5.5- TYPICAL DEFORMATION /PRESSURE TIME HISTORY EQUIPMENT OPENING RADIAL MOVEMENT

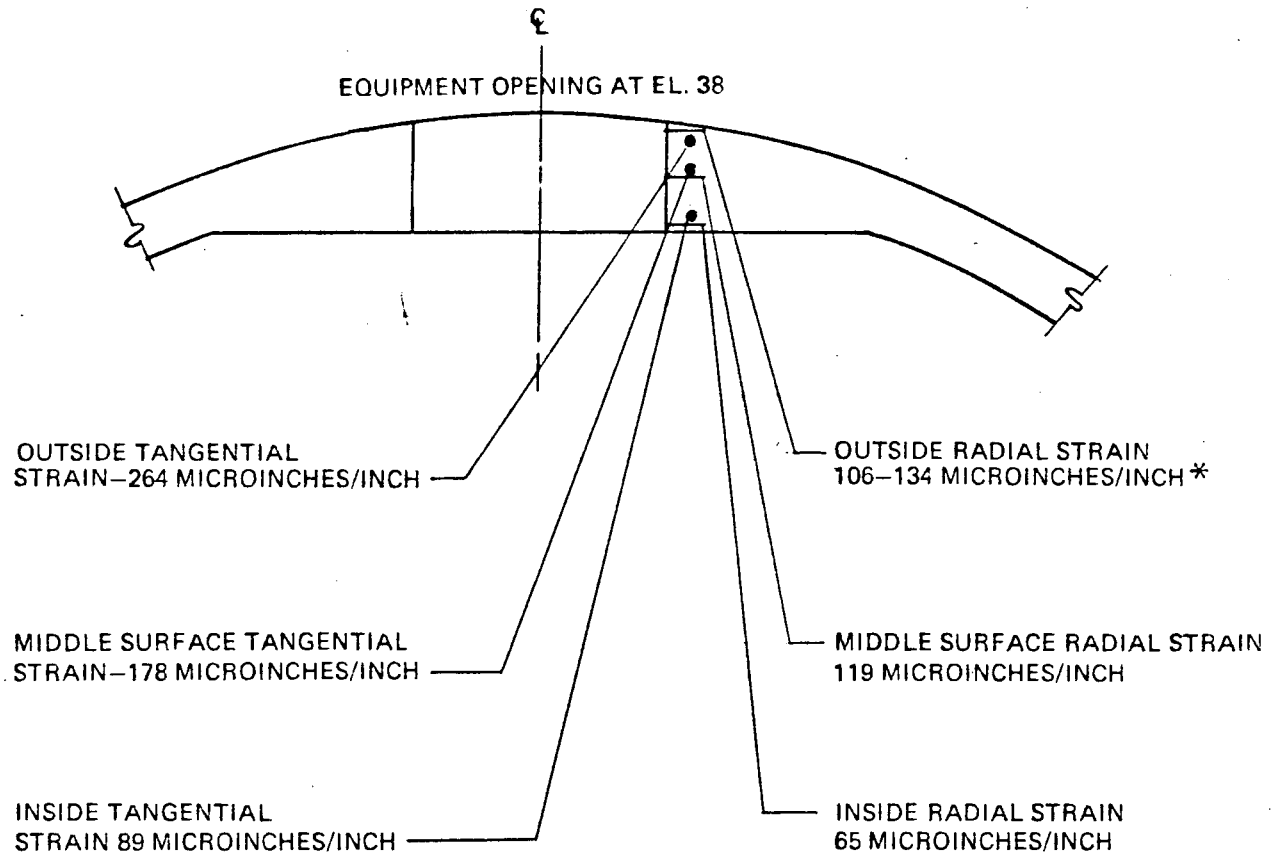

* MEASURED STRAINS AT 69 PSIG WERE
106 μ IN/IN AT START OF HOLD PERIOD
121 μ IN/IN ONE HOUR INTO HOLD PERIOD
134 μ IN/IN AT END OF TWO HOUR HOLD PERIOD
SENSOR ERRATIC THROUGHOUT TEST

FIGURE 5.6 - MEASURED CONCRETE STRAINS AT 69.4 PSIG EDGE OF EQUIPMENT OPENING

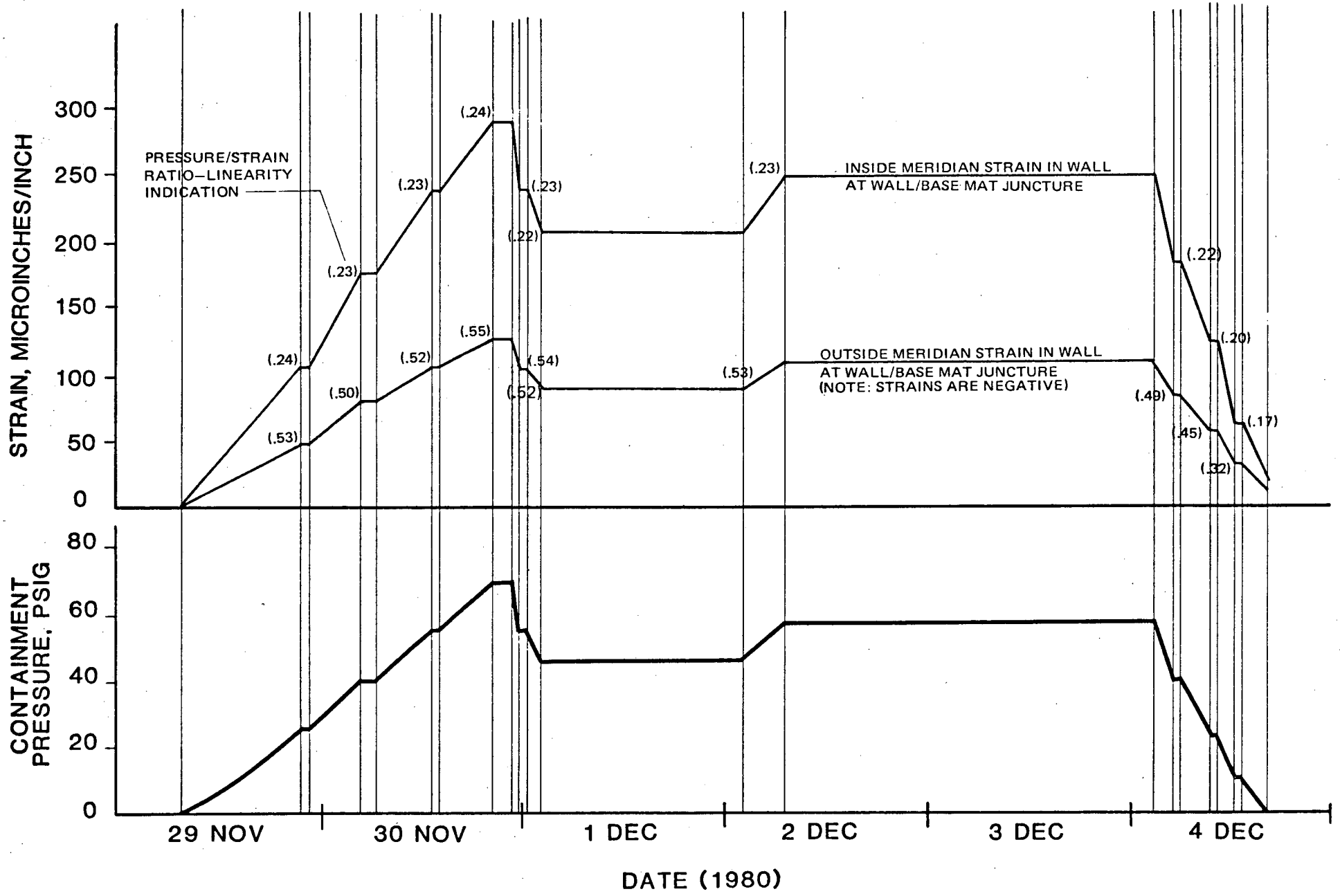

FIGURE 5.7 - TYPICAL STRAIN/PRESSURE TIME HISTORY BASE OF WALL

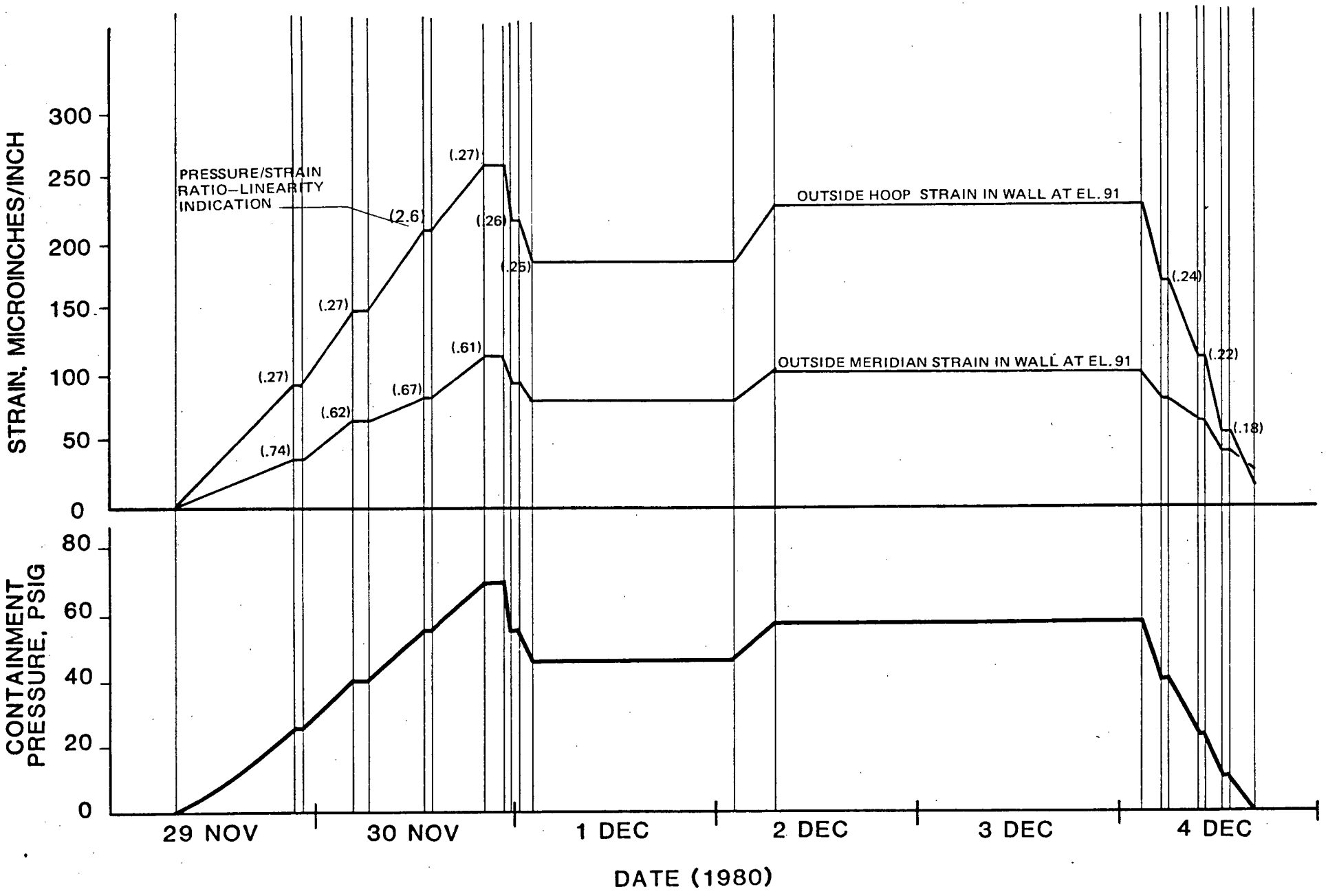

FIGURE -5.8 - TYPICAL STRAIN /PRESSURE TIME HISTORY WALL AT EL. 91

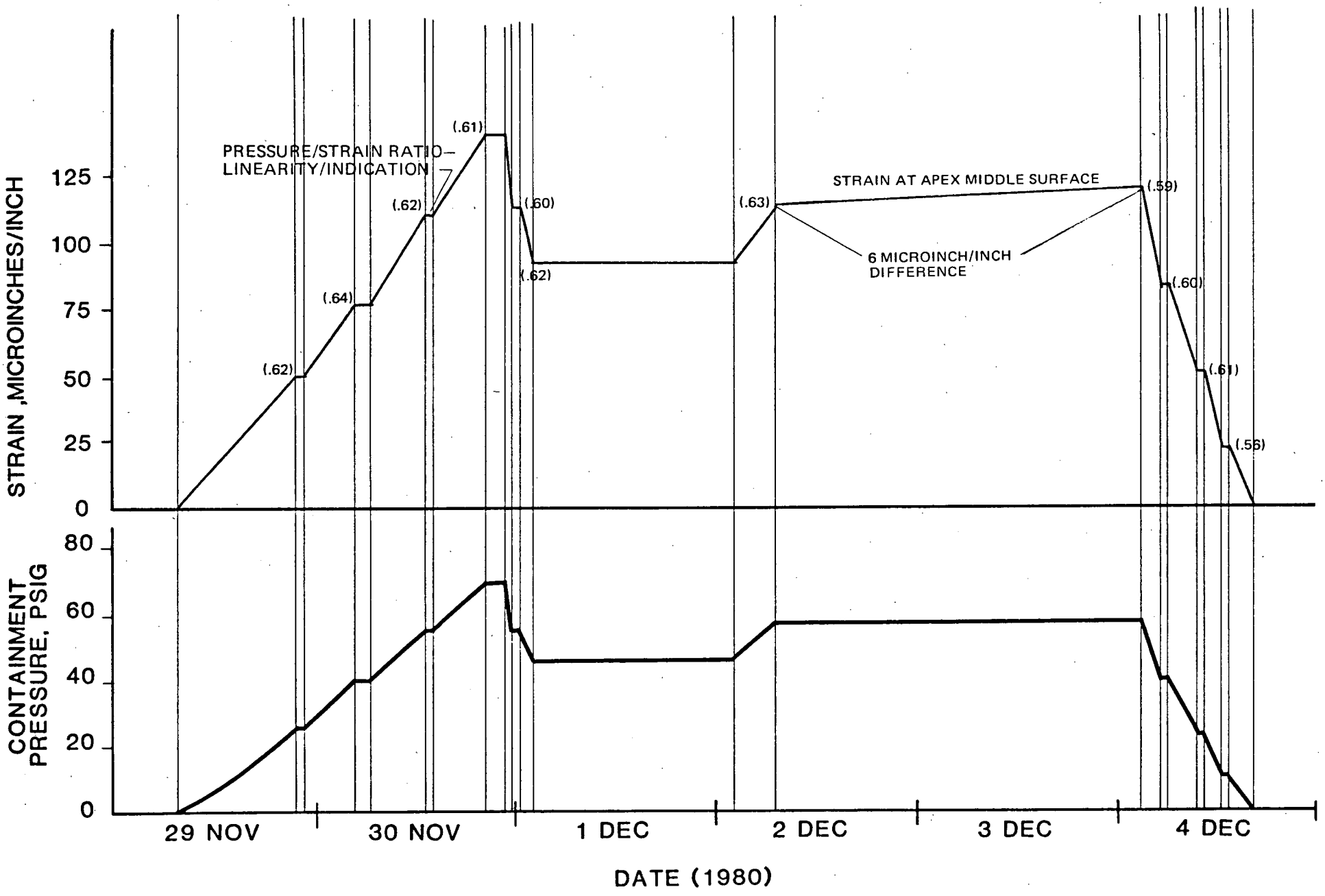

FIGURE 5.9 - TYPICAL STRAIN/PRESSURE TIME HISTORY DOME APEX

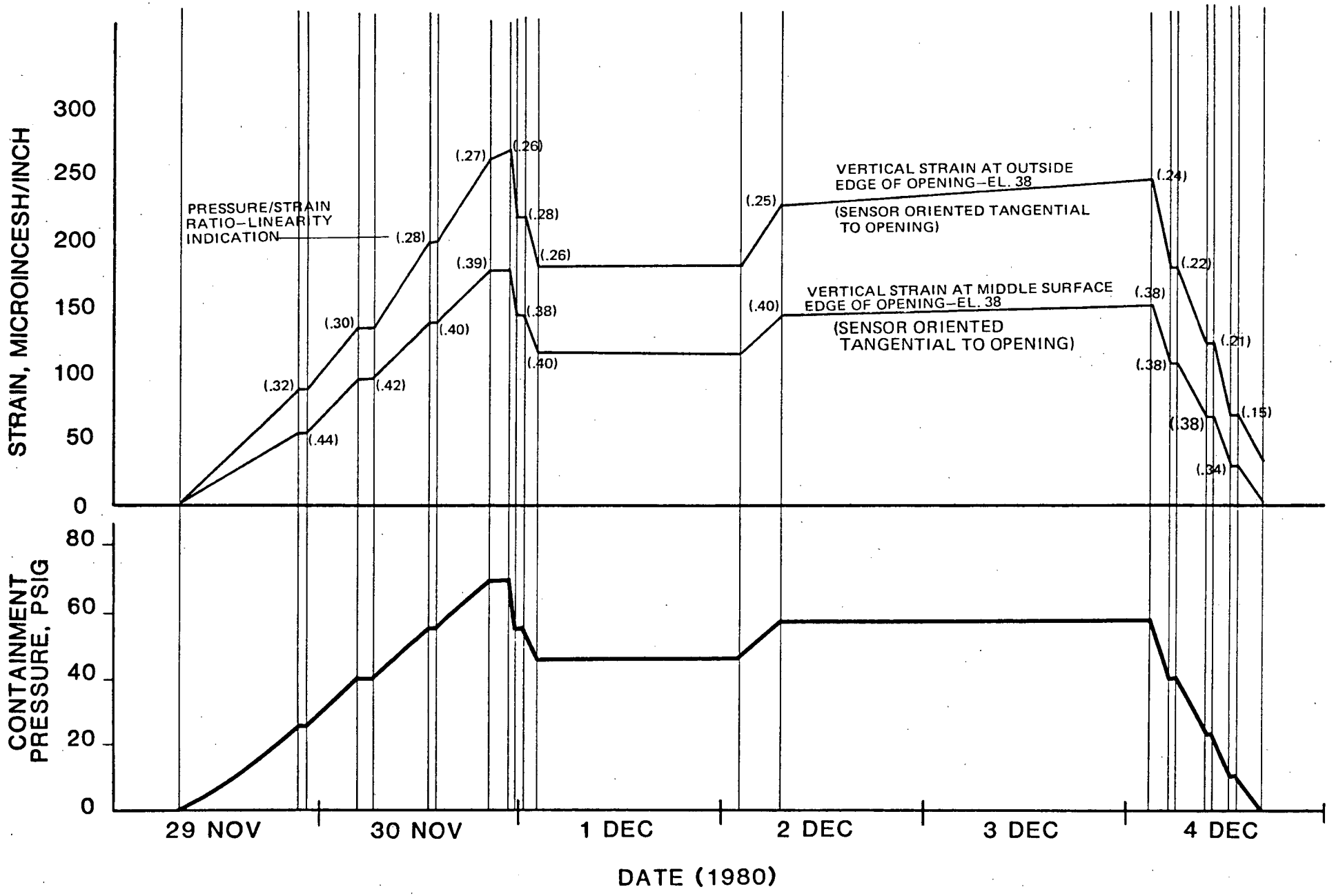

FIGURE 5.10 - TYPICAL STRAIN/PRESSURE TME HISTORY EQUIPMENT OPENING

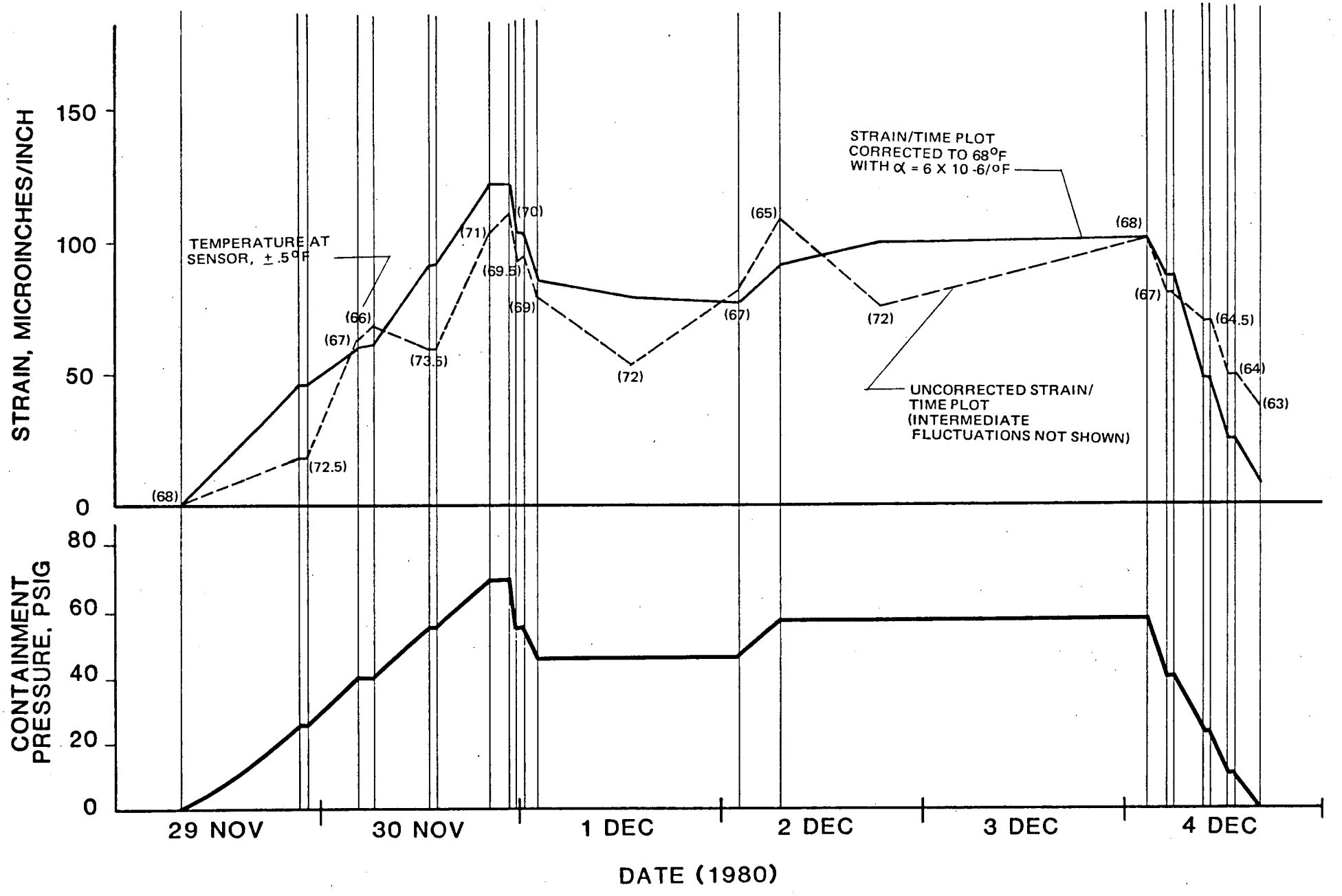

FIGURE 5.11 - STRAIN PRESSURE TIME HISTORY WITH TEMPERATURE CORRECTION OUTSIDE MERIDIAN STRAIN IN WALL AT SPRINGLINE

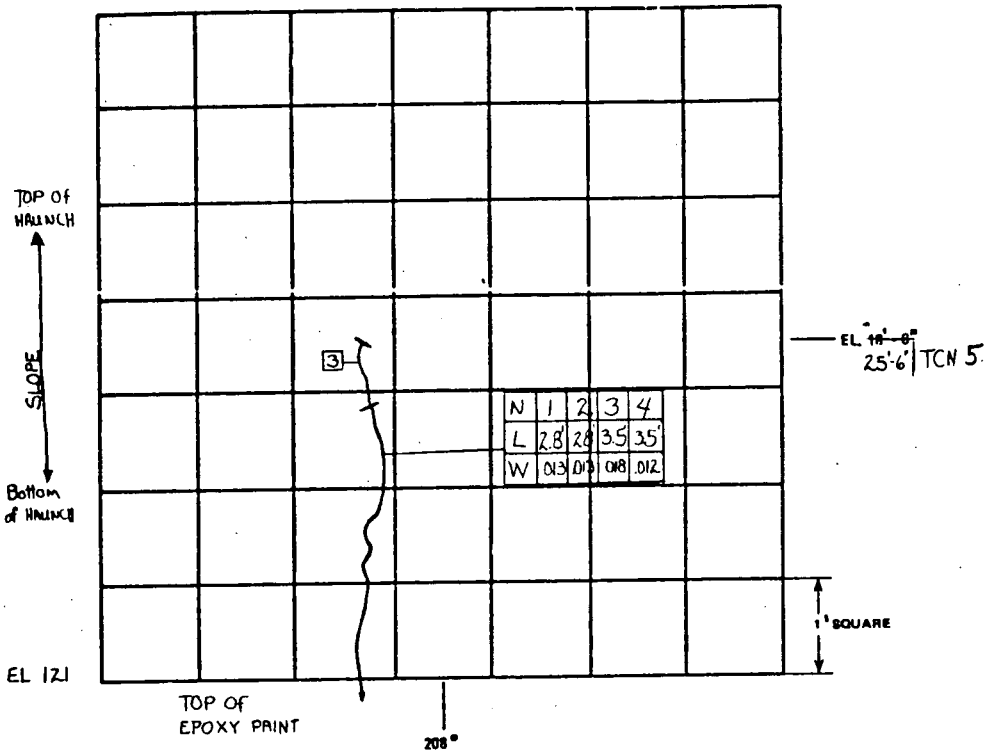

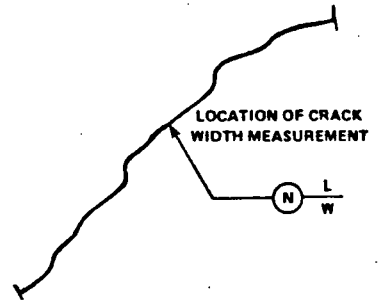

N = STAGE NUMBER
L = CRACK LENGTH IN INCHES
W = CRACK WIDTH IN INCHES

DATE	TIME	TEMP OF IN	TEMP OF OUT	STAGE	PSIG	BY	REMARKS
26 NOV 80	3:30 P	71	68	ONE	0	DRS NMH	O.P.* 1447
30 NOV 80	5:00 A	71	68	TWO	40	NMH DRS	O.P.* 1447
30 NOV 80	9:30 P	70	67	THREE	69	NMH DRS	O.P.* 1447
05 DEC 80	5:00 P	70	68	FOUR	0	NMH DRS	O.P.* 1447

OPTICAL COMPARATOR

Data Transcribed from Blueline sheets
12-24-80
Dave A Kasanovich 12/26/80
John T Kelly 12-26-80

FIGURE 5.12
CONCRETE SURFACE SURVEILLANCE AREA 1

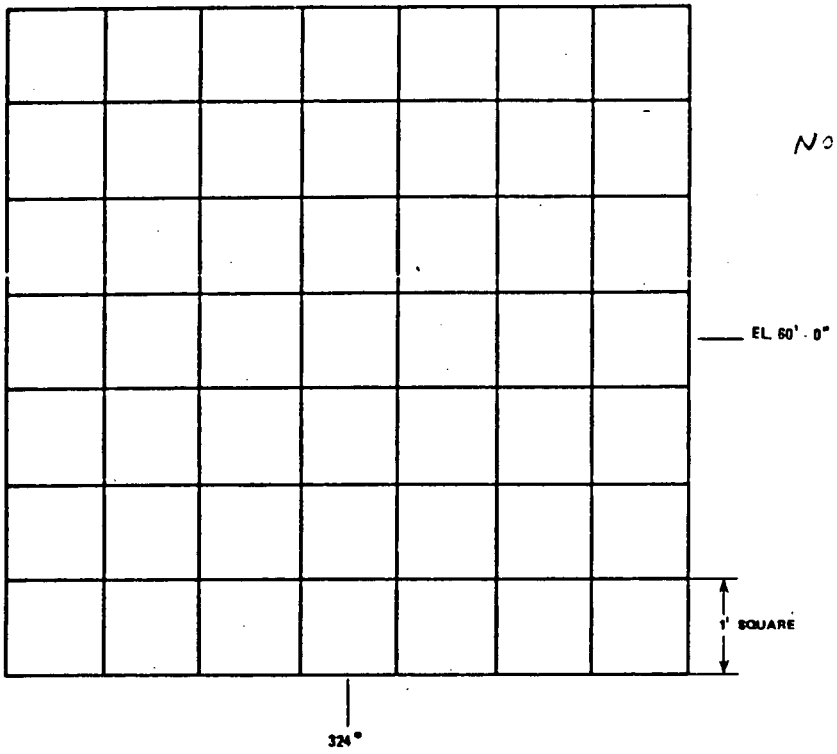

NOTE: NO CRACKS EXCEEDING .010 IN. OBSERVED AT ANY STAGE

2/24/81

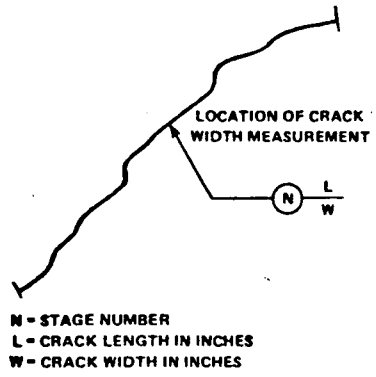

DATE	TIME	TEMP °F IN	TEMP °F OUT	STAGE	PSIG	BY	REMARKS
26 NOV 80	3:15 P	71	68	1	0	WH DN	OPTICAL COMPARATOR # 1451
30 NOV 80	05:25 A	70	67	2	40	WH DN	OPTICAL COMPARATOR # 1451
30 NOV 80	20:58	71	68	3	69	WH DN	OPTICAL COMPARATOR # 1451
05 DEC 80	16:50	71	68	4	0	WH DN	OPTICAL COMPARATOR # 1451

Data Transcribed From Blueline sheets
12-26-80
Dave A Zagorowich 12/26/80
Kelly 12-26-80

FIGURE 5.13
CONCRETE SURFACE SURVEILLANCE AREA 2

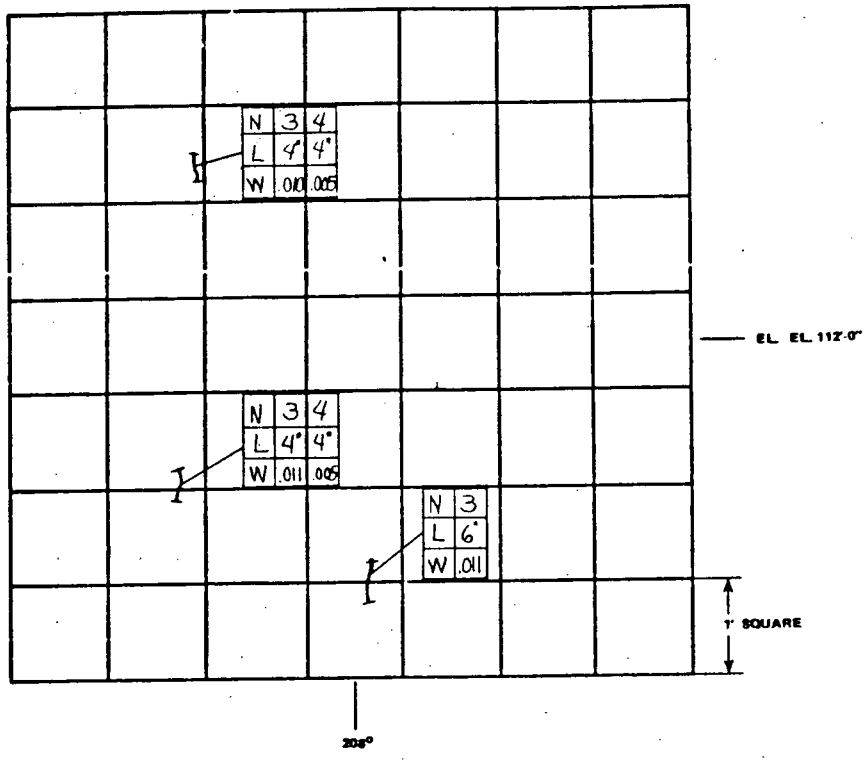

No cracks exceeding 10 mills were observed during stage one.

No cracks exceeding 10 mills were observed during stage TWO.

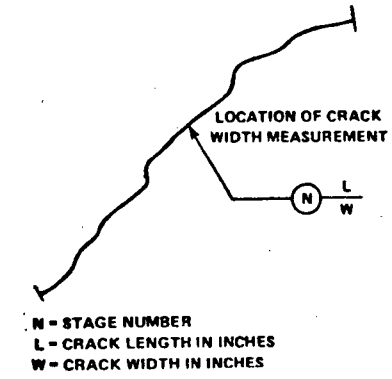

DATE	TIME	TEMP °F IN	TEMP °F OUT	STAGE	PSIG	BY	REMARKS
26 NOV 80	3:30 P	71	68	ONE	0	DRS NMH	O.P.* 1447
30 NOV 80	5:00 A	70	67	TWO	40	NMH DRS	O.P.* 1447
30 NOV 80	9:30 P	70	67	THREE	69	NMH DRS	O.P.* 1447
05 DEC 80	5:00 P	71	68	FOUR	0	NMH DRS	O.P.* 1447

OPTICAL COMPARATOR

Data Transcribed from Blueline sheets
12-26-80
Dave A Zagrocki 12/26/80
John T Kelly 12-26-80

FIGURE 5.14
CONCRETE SURFACE SURVEILLANCE AREA 3

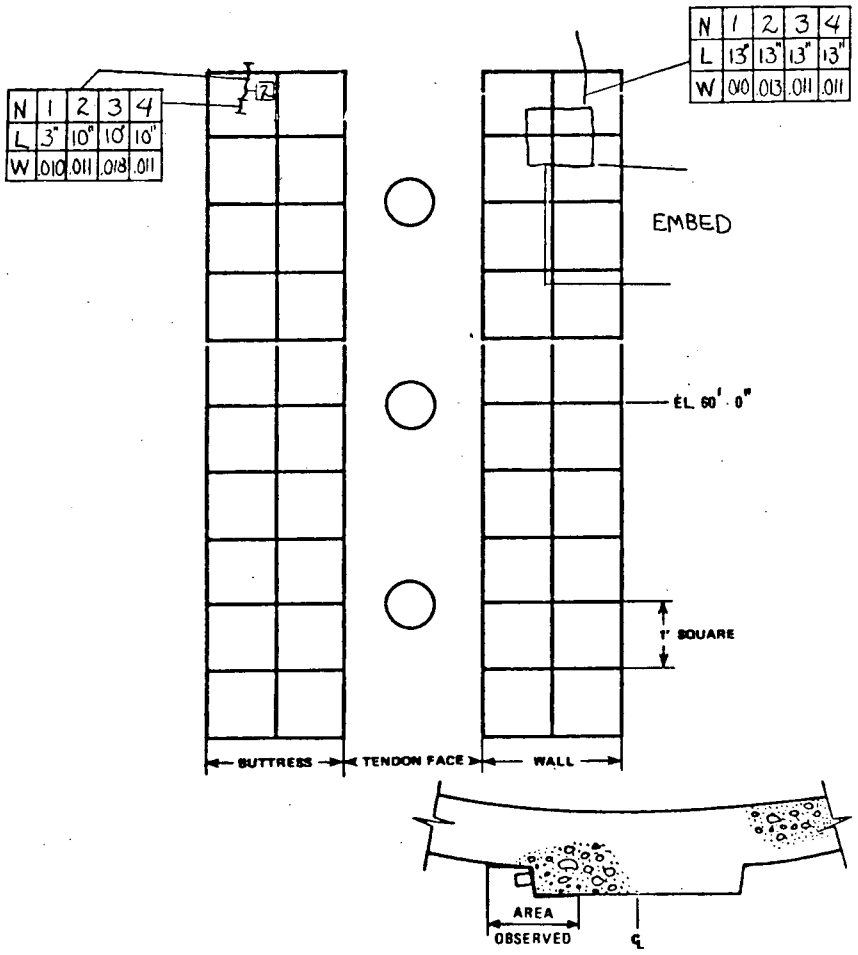

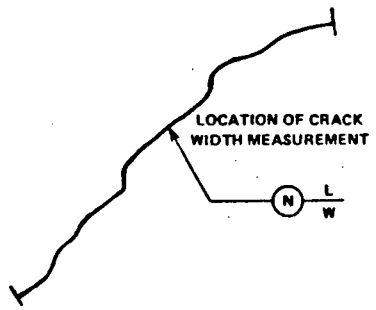

N = STAGE NUMBER
L = CRACK LENGTH IN INCHES
W = CRACK WIDTH IN INCHES

DATE	TIME	TEMP °F IN	TEMP °F OUT	STAGE	PSIG	BY	REMARKS
26 NOV 80	4:30 P	71	67	1	0	PHW DPC	COMPARATOR # 1443
30 NOV 80	5:45 A	70	68	2	40	PHW DPC	COMPARATOR # 1443
30 NOV 80	4:24 P	71	68	3	69	PHW DPC	COMPARATOR # 1443
05 DEC 80	5:50 P	70	67	4	0	PHW DPC	COMPARATOR # 1443

Data Transcribed from Blueline sheets
12-26-80
Dave A Zagarouski 2/26/80
John T Kelly 12-26-80

FIGURE 5.15
CONCRETE SURFACE SURVEILLANCE AREA 4

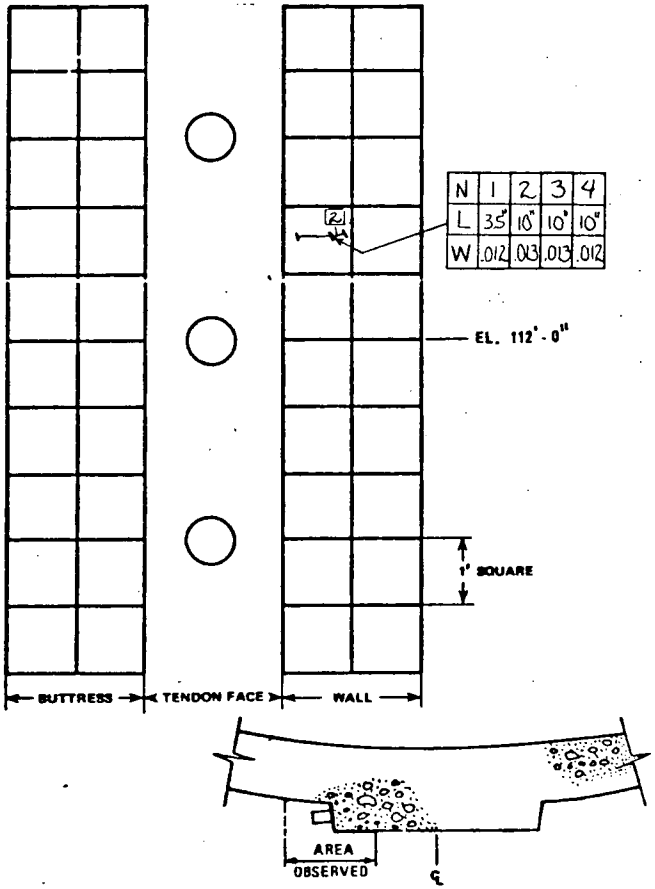

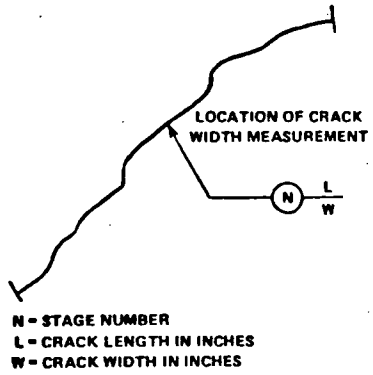

DATE	TIME	TEMP °F IN	TEMP °F OUT	STAGE	PSIG	BY	REMARKS
26 NOV 80	15:00	70	67	1	0	WH/DN	OPTICAL COMPARATOR* 1451
30 NOV 80	05:13	71	68	2	40	WH/DN	OPTICAL COMPARATOR* 1451
30 NOV 80	20:46	70	67	3	69	WH/DN	OPTICAL COMPARATOR* 1451
05 DEC 80	17:15	71	68	4	0	WH/DN	OTICAL COMPARATOR* 1451

Data Transcribed from Blueline sheets
12-26-80
Dave A Kasprowicz 12-26-80
John T Kelly 12/26/80

FIGURE 5.16
CONCRETE SURFACE SURVEILLANCE AREA 5

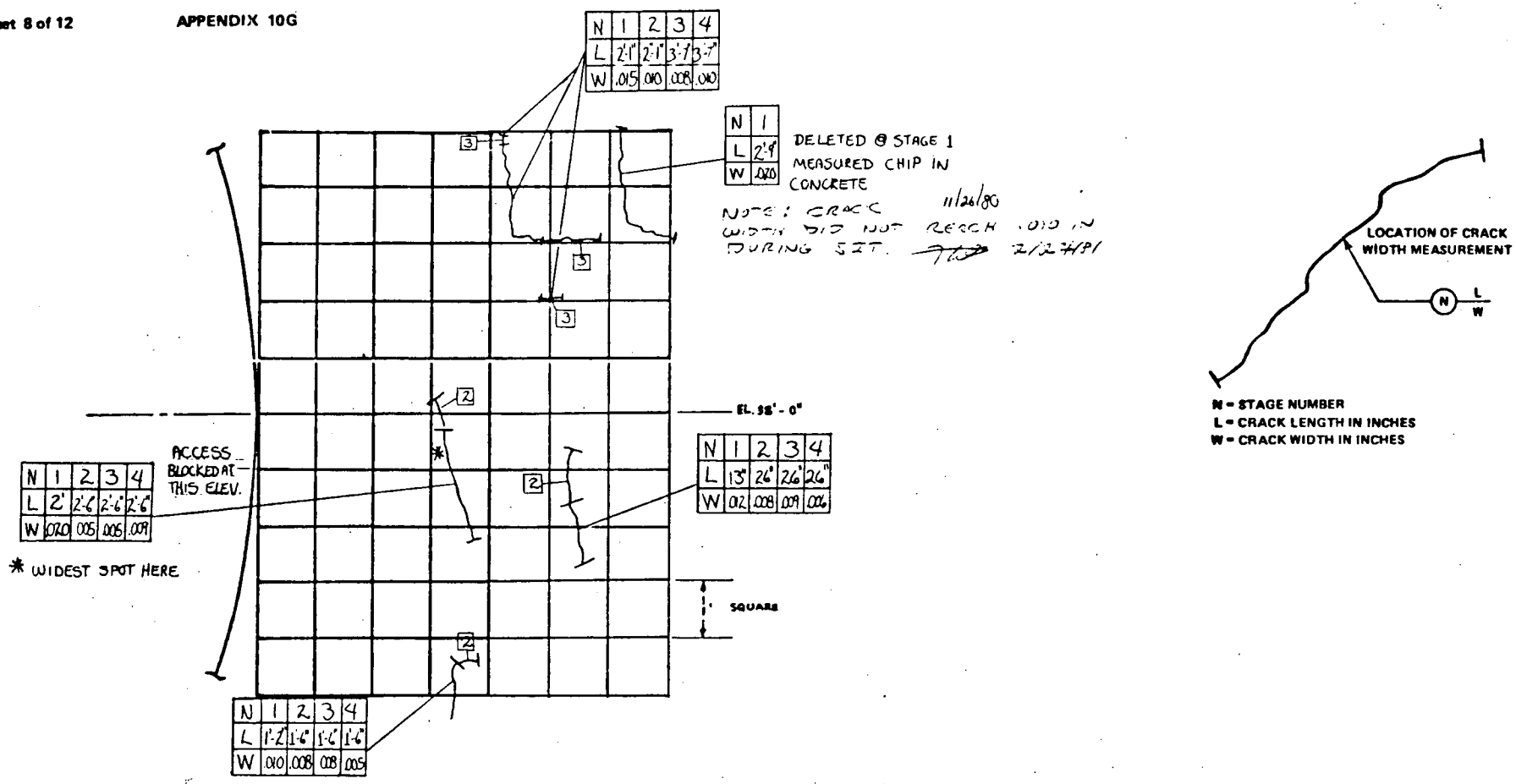

DATE	TIME	TEMP OF IN	TEMP OF OUT	STAGE	PSIG	BY	REMARKS
26 NOV 80	09:30	70	67	1	0	PHW DFC	COMPARATOR #1443
29 NOV 80	05:45	70	68	2	40	PHW DFC	COMPARATOR #1443
30 NOV 80	9:24	71	67	3	69	PHW DFC	COMPARATOR #1443
05 DEC 80	5:50	70	68	4	0	PHW DFC	COMPARATOR #1443

Data Transcribed from Blueline sheets
12-26-80
Dave A Yasenovec 12/26/80
John T Kelly 12-26-80

FIGURE 5.17

CONCRETE SURFACE SURVEILLANCE AREA 6

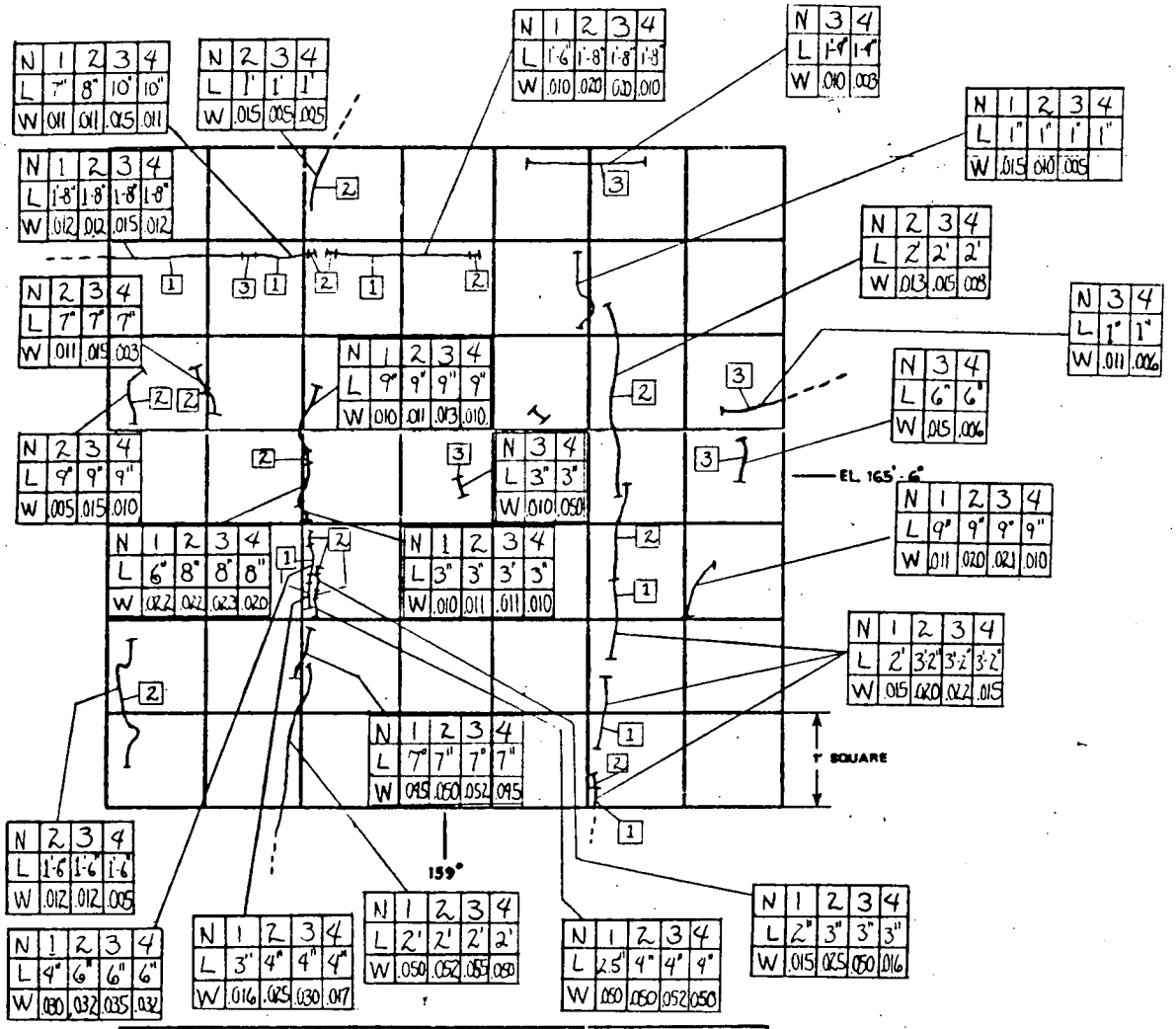

DATE	TIME	TEMP °F IN	TEMP °F OUT	STAGE	PSIG	BY	REMARKS
26 NOV 80	2:30 P	70	68	1	0	SY	O.P. * SU1446
29 NOV 80	9:30 A	70	68	2	40	SY	O.P.* SU1446
30 NOV 80	8:25 P	70	67	3	69	SY FMD	O.P.* SU1446
05 DEC 80	4:15 P	71	68	4	0	SY HNN	O.P.* SU1446

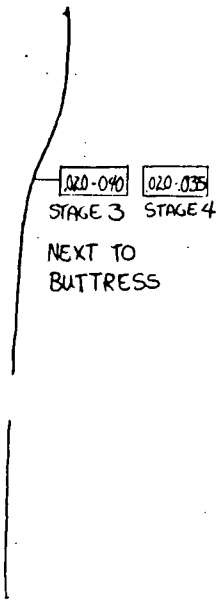

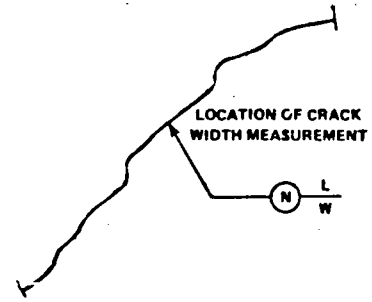

DATA TRANSCRIBED from Blueline sheets
12-26-80
Dave A Hoornaert 12/26/80
12-26-80

FIGURE 5.18
CONCRETE SURFACE SURVEILLANCE AREA 7

6. REFERENCES

a. San Onofre Nuclear Generating Station, Unit 2, Primary Reactor Containment Structural Integrity Test Procedure, 2 PE-101-03, Revision 0.

b. San Onofre Nuclear Generating Units 2 and 3, Final Safety Analysis Report.

c. United States Nuclear Regulatory Commission Regulatory Guide 1.18, Structural Acceptance Test for Concrete Primary Reactor Containments, Revision 1.

d. BC-TOP-5, Prestressed Concrete Nuclear Reactor Containment Structures, Revision 1, Bechtel Corporation, December, 1972.